Synthesis, Characterization and Application of Selected Nanocatalysts in Wastewater Treatment

Researchers
Name: Sabahat Saleem

Reg # 196-FBAS/MSES/S14

Supervisor
Name: Dr.Faiza Jan Iftikhar

Designation: Assistant professor

Co Supervisor
Name: Dr.Muhammad Irfan
Designation: Assistant professor (NCP)

Department of Environmental Sciences

Faculty of Basic and Applied Sciences

International Islamic University Islamabad

(2017)

MS
541.395
SAS

Catalysis
X-Ray diffraction

Synthesis, Characterization and Application of Selected Nanocatalysts in Wastewater Treatment

Researchers
Name: Sabahat Saleem

Reg # 196-FBAS/MSES/S14

Supervisor
Name: Dr.Faiza Jan Iftikhar

Designation: Assistant professor

Co Supervisor
Name: Dr.Muhammad Irfan
Designation: Assistant professor (NCP)

Department of Environmental Sciences

Faculty of Basic and Applied Sciences

International Islamic University Islamabad

(2017)


بسم الله الرحمن الرحيم

Department of Environmental Sciences
International Islamic University, Islamabad

Dated: _____

Final Approval

It is certified that we have read the project report submitted by the Sabahat Saleem. It is our judgment that this project is of sufficient standard to warrant its acceptance by the International Islamic University, Islamabad for the Master Degree in Environmental Sciences.

Examination Committee

External Examiner

_____

Internal Examiner

_____

Supervisor
Dr.Faizan Jan Iftikhar
Assistant Professor
Department of Environmental Sciences
International Islamic University, Islamabad

_____

Co-Supervisor
Dr.Muhammad Irfan
Assistant Professor
NCP, QAU Campus, Islamabad

_____

Acting Chairperson
Dr.Rukhsana Tariq
Department of Environmental Sciences
International Islamic University, Islamabad

DR. RUKHSANA TARIQ
A.Chairperson
Department of Environmental Science
International Islamic University Islamabad

_____

Dean, FBAS
Professor Dr. Muhammad Arshad Zia
International Islamic University, Islamabad

_____

Dy.No 268 Date 8/8/2017
Chairperson Office
DES

A thesis submitted to Department of Environmental Sciences,
International Islamic University, Islamabad as a partial
fulfillment of requirement for the award of the
degree of MS. Environmental Sciences.

FORWARDING SHEET

The thesis entitled ''Synthesis, Characterization and Application of Selected Nanocatalysts in Wastewater Treatment'' submitted by Sabahat Saleem in the partial fulfillment of MS Environmental Sciences has been completed under my supervision and guidance. I am satisfied with the quality of the student's research work and allow her to submit it for further processes as per IIUI rules and regulations.

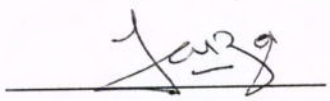

Dr. Faiza Jan Iftikhar

DEDICATION

Dedicated to my beloved parents and siblings for their immense support for this achievement and my teachers for their proper guidance and to all those who shared their knowledge.

DECLARATION

I hereby declare that the work present in the following thesis is my own effort, except where otherwise acknowledged and that the thesis is my own composition. No part of the thesis has been previously presented for any other degree.

Date Sabahat

Sabahat Saleem

CONTENTS

ACKNOWLEDGEMENTS

First of all, I offer my deepest gratitude to **ALLAH ALMIGHTY**, Who has given me strength and courage to complete my research work. His help was always there to help me in my critical moments. I am really thankful to my Creator.

I owe my special thanks to my supervisor, **Dr. Faiza Jan Iftikhar** for her co-operative behavior, continuous support and guideline throughout my research write up.

I want to express my heartiest gratefulness to my Co-supervisor, **Dr. Muhammad Irfan** for his whole hearted assistance, valuable suggestions and worthy guidance during my whole research study and write up.

I am also thankful to **International Islamic university, Islamabad** which provided me the pathway for my studies and also a bundle of thanks to **National Centre for Physics (NCP), Islamabad,** to carry out my research work.

I am pleased to express special thanks to my **friends** for their help, moral support and encouragement during my study.

Finally, I pay deepest regards to my **Parents** for their endless love, support, motivation and encouragement at each and every step during the extent of my education and research work. I am also thankful to all other family members especially my **brothers (Asad, Basit & Sheri)** for their help when required. Without their co-operation it was impossible for me to do this research in even way. I am highly beholden to them for everything.

Sabahat Saleem

LIST OF ABBREVIATIONS

UNIDO	United Nation Industrial Development and Organization
UNWWAP	United Nations World Water Assessment Programme
WHO	World Health Organization
UNCIF	United Nation Children's Fund
WB	The World Bank
NCP	National Centre for Physics
NS & TD	Nanoscience and Technology Division
QAU	Quaid-i-Azam University
nm	Nanometer
NPs	Nanoparticles
mg	milligram
ml	milliliter
mM	millimolar
µl	microliter
cm	centimeter
g	gram
rpm	Rosultion per minute
°C	Celsius scale
pa	Pascal
λ	Lambda
%	percent
MB	Methylene Blue
MO	Methyl Orange
CR	Congo Red
CV	Crystal Violet
4-NP	4-Nitrophenol
-NO3	Nitro group
-N=N-	Azo group
$-NH_2$	amino group

H_2O_2	Hydrogen peroxide
NaBH4	Sodium borohydride
$OH^{\bullet}$	Hydroxyl radicals
rGO	Reduced Graphene Oxide
GO	Graphene oxide
CuO	Cupric oxide
Cu_2O	Cuprous oxide
Au NPs	Gold nanoparticles
PAMAM	Polyamido amine
CTAB	Cetyl trimethylammonium Bromide
SDS	Sodium dodecyl sulphate
PEG	Polyethylene glycol
PVP	Poly vinyl pyrolidine
CN	Cellulose Nanocrystals
γ-Al_2O_3	Gamma alumina
AlOOH	aluminium oxide hydroxide
$Cu(NO_3)_2.3H_2O$	Copper Nitrate. trihydrate
$Co_2(NO_3).6H_2O$	Cobalt Nitrate Hexahydrate
$CO(NH_2)_2$	Urea
NH_4OH	Ammonia solution
N_2H_4	Hydrazine Hydrate
C_2H_5OH	Ethanol
C_3H_6O	Acetone
Cu/Al_2O_4	Copper/alumina
CO/Al_2O_4	Cobalt/alumina
HDP	Homogenous Precipitation Deposition method
XRD	X-ray Diffraction
JCPDS	Joint Committee on Powder Diffraction Standards
ICDD	International Centre for Diffraction Data
SEM	Scanning Electron Microscopy
TGA	Thermogravimetric analysis

ABSTRACT

Organic dyes and nitro aromatic compound are the most commonly used industrial chemicals which are toxic (carcinogenic and mutagenic) in nature, and their complex synthetic structure makes their degradation a difficult task. Recent advances in nanotechnology offer great opportunities in solving existing water pollution problems by providing variety of nanomaterials which exhibit unique phenomena that enable novel applications including high surface area for adsorption, high activity for catalysis, and other unique optical and electronic properties that find use in new treatment processes and sensors for water quality monitoring. Recently, researchers have found that metal nanoparticles and their oxides show high catalytic activity for the chemolysis of environmental pollutants.

In the present study, we have successfully synthesized CuO NPs using an easy and environmentally benign chemical reduction method and γ-alumina based copper and cobalt nanocomposites were fabricated *via* Homogenous Deposition Precipitation (HDP) method in aqueous media. The as-prepared samples were characterized using different analytical techniques such as X-ray Diffraction (XRD), Scanning Electron Microscopy (SEM), Thermogravimetry analysis (TGA). Subsequently, the catalytic activity of unsupported and supported metal nanocatalyts was investigated against organic dyes (Methylene Blue and Methyl Orange) and other organic pollutant (4-Nitrophenol) for their oxidative and reductive degradation. The progress of catalytic reactions was monitored using UV/vis spectrophotometer.

Oxidation of dye molecule was carried out in the presence of hydrogen peroxide (H_2O_2) as green oxidant while sodium borohydride ($NaBH_4$) was used as reducing agent in the reduction reactions. The prepared nanocatalyst showed excellent catalytic activity for the degradation of organic environmental pollutants (Methylene Blue, Methyl Orange and 4-Nitrophenol). In case of catalytic oxidative degradation, better decomposition was observed for Methylene Blue in the order of 60% > 50% = 40% with Cu/Al_2O_4, Co/Al_2O_4 and CuO NPs respectively. On the other hand, Methyl Orange was selected for reductive

degradation which was as high as 100 % within 5 minute. 4-nitrophenol was completely reduced into 4-aminophenol with 60 second in the presence of $NaBH_4$.

The possible mechanism behind the oxidative degradation is the generation of hydroxyl radical by the decomposition of H_2O_2 that is capable of reacting with the variety of organic compound leading to either partial or complete degradation. In the reduction reactions, nanocatalyst facilitate the electron transfer from hydride ion to azo group (-N=N-) of the dye molecule which thus undergoes reduction and decomposition to give nontoxic products with amine group ($-NH_3$). The results confirmed the high catalytic activity of the prepared nanocatalysts for the degradation of azo dyes and 4-nitrophenol. As the supported nanocatiysts are prepared in a reliable and cost effective method so can be applicable for the industrial-scale removal of the azo compounds pollutant from the wastewater streams.

CHAPTER # 1

INTRODUCTION

Introduction

1.1. Background/Motivation

Water is the most valuable entity for the survival of life on earth. Access to safe and clean water (i.e., free from toxic chemicals and pathogens) is not only a basic human need; but is also essential for proper functioning of ecosystems, communities and economies. It is estimated that nearly 1.4 trillion Cubic meter of water is present on earth, of which only 1% (surface and groundwater resources) is available to meet all human requirements. Due to rapid increase in urbanization and environmental pollution, the available freshwater is being contaminated with toxic substances that ultimately result in economic and health crises (Tahir et al., 2010).

Ensuring reliable access to clean and affordable water is one of the greatest global challenges of this century. About 1.1 billion people are without sufficient access to water, and 2.5 billion people have to live without adequate sanitation (UNICEF & WHO, 2008). The World Health Organization (WHO) has estimated that worldwide, 80% of illnesses in the developing world are due to water-borne diseases (WHO, 2002).

According to World Bank Report, there are 17 countries including Pakistan that are facing water shortage problem. It is estimated that 44% of population in Pakistan is without access to safe drinking water. In rural areas, up to 90% of the population lacks such access. Furthermore, it is estimated that about 200,000 children in Pakistan die every year because of diarrheal diseases alone (UNIDO, 2003).

There are many natural and human processes that affect the water quality by changing its physical and biochemical characteristics. Continued disposal of untreated municipal, sewage and industrial waste leads to addition of toxic organic and inorganic contaminants in both surface and ground water throughout the world (MA, 2005a). Nutrient and pesticide contamination is mainly contributed by the agriculture sector. Every day, 2 million tons of sewage, industrial and agricultural waste is discharged into the world's water (UNWWAP, 2009).

Industrialization has been swift usually at the expense of over-exploiting and polluting the environment, especially the aquatic one, because the wastewater released from the industries contain a high concentration of organic and inorganic pollutants (Hu et al., 2015). Industrial activity disposes about 300-400 million tons of heavy metals, solvents, toxic sludge and other organic waste into world's water each year (UNWWAP, 2015). Amongst the entire industrial sector, textile effluent has received worldwide attention in the recent years because of its considerable amount and toxicity (Chequer et al., 2013). The World Bank (WB) estimates that 17-20% of industrial water pollution is constituted of textile synthetic dyes and pollutants (Zhou et al., 2010). Due to the incompetence of dyeing processes, upto 200,000 tons of these dyes are lost to effluents per year during the dyeing and finishing operations in waterways (Ogugbue & Sawidis, 2011).

Significant amount of wastewater discharged by textile industry contains high content of residual pollutants such as aromatic compounds including different kinds of dyes and nitro compounds even after post-treatment by conventional methods. Among the aromatic pollutants, water pollution due to organic dyes is of the major environmental concern because trace quantity of these is not only highly visible but also affects the aesthetic quality and transparency of water bodies (Gosh et al., 2015).

Dyes are the substances that impart color to the substrate having great use in our daily life (Bafana et al., 2011). These are widely employed in the traditional textile industry as well as in industries like food, cosmetics, therapeutic products, solar cells and optical data disc. Dyes are classified according to their application and chemical structure. All dyes are basically composed of the organic compound, a group of atom responsible for dye color (chromophores) and an electron withdrawing and donating substituent that cause or intensify the color of the chromophores called auxophores. The most important chromophores are azo (-N=N-), carbonyl (-C=O-), methane ($-CH_3=$), nitro ($-NO_2$) and quinoid groups. The most important auxophores are amine ($-NH_3$), carboxyl (-COOH), sulphonate ($-SO_3H$) and hydroxyl group (-OH) (Prasad& Rao, 2010). In the organic dyes, the azo group (-N=N-), aromatic ring and auxochromes combine in such a way that makes the dye molecule toxic, and stable towards biodegradation (Zhang et al., 2011).

Azo dyes constitute about 60-70% of all the coloring agents worldwide (Carliell et al., 1998).

Unfortunately, organic compounds (dyes and nitro aromatics) are easily soluble in water and hard to be self-cleaned by the environment. Thus, poses serious and long term threat to aquatic ecosystem (plants, micro-organism and animals) as colored wastewater inhibits the sunlight penetration and render dissolved oxygen required for efficient photosynthesis in aquatic plants. Most of the aromatic pollutants threaten the lives on land including human by creating acute toxicity as organic azo dyes are carcinogenic and mutagenic in nature because of their non-biodegradability properties (Yang et al., 2010).

Methylene blue (MB) $C_{16}H_{18}N_3SCl$ is a polyaromatic synthetic dye with the molecular weight of 319.85g/mol. It imparts deep blue color to the substance and dissociates into cations and chloride anions when dissolved in water (Rafatullaha et al., 2010). It is commonly used as basic cationic dying material for wood, silk, and cotton (Hameed et al., 2007). Additionally, Methyl orange (MO) $C_{14}H_{14}N_3NaO_3S$ is the acidic anionic azo dye with molecular weight of 327.33g/mol (Ai et al., 2011). Acute exposure to these dyes can cause increased heart rate, vomiting, shock, cyanosis, jaundice, gastrointestinal problems and tissue necrosis in humans (Yi et al., 2008).

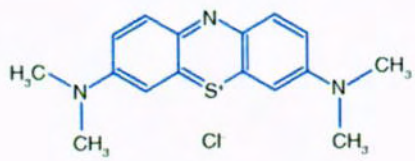

Methylene Blue

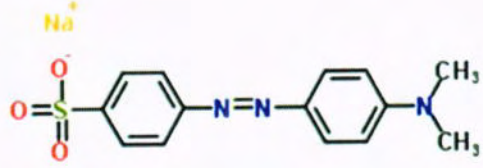

Methyl Orange

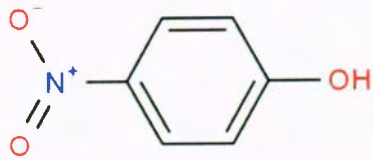

4-nitrophenol

On the other hand, Nitro aromatic compounds are the largest and most important toxic derivative of parathion insecticide. It is carcinogenic and mutagenic to mammals. These compounds are the class of organic molecules that consist of one or more than one nitro

group (-NO_2) attached to an aromatic ring. Combination of two electron-deficient oxygen atoms with partially positive nitrogen atom makes the nitro group more electronegative in nature and when combined with benzene ring, it makes nitro group an important functional group for chemical synthesis (Ju & Parales, 2010).

However, many water soluble aromatic compounds undergo structural changes due to their complex structure and synthetic origin which makes them recalcitrant towards conventional wastewater remediation technologies (Hu et al., 2015).

Several physico-chemical and biological techniques such as adsorption, photodegradation, bio-degradation, reverse osmosis, desalination have been developed and applied during the last few decades (Xu et al., 2014), But these conventional treatment methods have proved to be inefficient to completely treat wastewater because of their high cost, low-efficiency and most of them produce toxic by-products post degradation (Simsikova et al., 2015). Thus, conventional treatment technologies have to be modernized, either updated or modified or replaced by developing materials and methods which are proficient, cost-effective, reliable and environmental friendly.

1.2. Nanotechnology: a sustainable alternative for wastewater treatment

Recent advances in nanotechnology offer great opportunities in solving existing water pollution problems both by enhancing the performance of existing treatment processes and developing new nanomaterials. The idea of nanotechnology was proposed in 1959 by *Richard Feyman* in often cited lecture *"there's plenty of room at the bottom"* (Miyazaki et al., 2007). The exact term was used by *Norio Taniquichi* in 1974, to explain semiconductor processes involving control of the order of nanometer. The essence of Nanotechnology lies in creating and manipulating the objects at dimensions of roughly 1 to 100 nanometers, i.e, size scale between individual atoms and bulk materials, where

unique phenomena of high surface to volume ratio enable novel applications (Theron et al., 2008). A nanometer is one-billionth of a meter. (Figure.1.1)

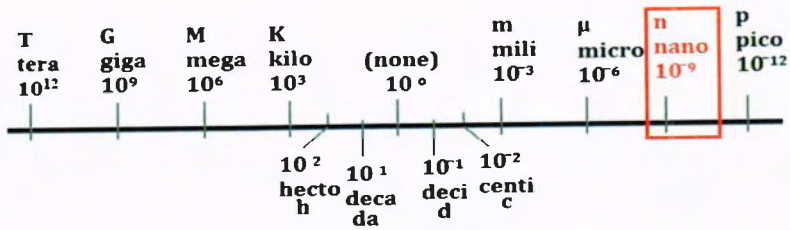

Figure.1.1. Relative size scale of length

Figure 1.2 displays the comparison of different things on the nanometer scale between 1 and 100nm. Things are so small at this level and are unique due to their large surface to volume ratio. A better idea comes from the diameter of pencil tip which accounts for about 1million of nanometers and a bacterium cell has around 10.000 nanometer size.

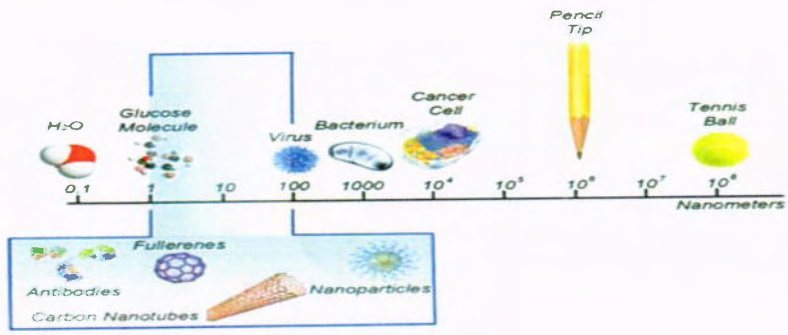

Figure.1.2. Size comparison on nanometer scale

In the field of environmental remediation alone, nanotechnology serves by providing nanomaterials that will enable new ways of waste minimization, using water and energy resources more sparingly, treating of industrial contamination, providing clean water, and improving the means of energy production and use (Bottero et al., 2005). These new materials owing to their small size are more reactive and their high surface area for chemical interaction has great potential to both revolutionize and challenge the current water treatment processes by developing new technologies for treating water and monitoring compounds (Chirag, P. 2015).

Nanomaterials have received much attention for their application in wastewater treatment because they possess high surface area for adsorption such as carbonaceous materials, high activity for catalysis such as metal oxide based nanocatalyts, and other unique optical and electronic properties that find use in novel treatment processes and sensors for water quality monitoring (Khin et al., 2012). Catalytic oxidation and reduction to mineralize or transform organic pollutant into non-toxic product is a matter of great interest. It deals with relatively green processes which are cost-effective, simple and highly efficient in handling the significant quantity of organic pollutants especially, organic dyes and nitro compounds.

Catalytic advanced oxidation in the presence of hydrogen peroxide (H_2O_2) is receiving more attention because H_2O_2 is an environmental-benign, greener oxidant that generates in situ hydroxyl radicals ($OH^{\bullet}$) that are capable of reacting with a variety of organic pollutants leading to their partial or complete degradation (Zhu et al., 2013). In addition, degradation of organic pollutants by catalytic reduction reaction represents an important class of fast, simple and low cost environmental technologies. It is easy to implement on an industrial scale, dye removal (Sha et al., 2016) in the presence of cost-effective and mild reducing agent such as sodium borohydride in which nanocatalysts facilitate the electron transfer from borohydride ions to azo group (-N=N-) of the dye molecule which thus, undergo reduction and decomposition to give non-toxic amino products (Chakravarty et al., 2015).

Recently, researchers have found that metal nanoparticles and their oxides could be used as effective catalysts for the chemolysis of environmental pollutants, for example, metal oxides (Au, Ag, Cu, Co and Ni) as nanocatalysts to reduce nitrophenols to aminophenols, and have received extensive attraction universally due to their proficient catalytic performance in aqueous media (Wu et al., 2015).

A research was conducted by Simsikova and co-workers in 2015, where they successfully synthesized gold nanoflowers (Au NFs) supported on reduced graphene oxide (rGO) *via* polyphenols extracted from green tea extract. The as prepared nano composite was

investigated for degradation of three azo dyes namely; safranine T, eosine Y and congo red in the presence of sodium borohydride ($NaBH_4$) with light irradiation. The results show short time intervals for complete degradation of azo dyes for example, it required 10 minutes for safranine T, 18 minutes for eosine Y and 26 minutes for congo red. They concluded that synthesized nanocatalyst acts as an excellent electron donor from BH_4^- to dye molecule that finally helps in chemical bond cleavage of the dye molecule.

Wang et al., 2015 found gold nanoparticles (Au NPs) supported on N-containing polymer sphere as an excellent catalyst for catalytic reduction of 4-nitrophenol into 4-aminophenol. The nanocomposite was synthesized through an in situ reductive growth process. In another study, silver and gold nanoparticles were immobilized onto graphene oxide (GO) functionalized with Polyamidoamine (PAMAM) dendrimers and tested for the catalytic reduction of azo dyes namely, Methyl Orange and Congo Red in the presence of $NaBH_4$. Results showed remarkable catalytic activity as both dyes reduced to non-toxic amino products within short reaction times (Rajesh et al., 2014).

A lot of studies have been reported on the catalytic activity of noble metal nanoparticles but these are expensive and scarce to be widely used (Wu et al., 2015; Hildebrand et al., 2009; Ma et al., 2015).

In fact, Mott and co-workers in 2007 found that transition metal oxides such as copper and cobalt oxide nanoparticles dominate over the use of expensive noble metals (Au, Ag, Pd and Pt), because they offer cheap alternative with broad potential applications in catalytic reactions (Deka et al., 2016) due to their environmental compatibility and quick accessibility (Sarkar & Dolui, 2015). Nanoscale synthesis of copper oxides and cobalt oxide (Co_2O_3) nanocatalysts is receiving extensive attention for their application in wastewater treatment.

Cupric oxide (CuO) is an environment-friendly, non-toxic and cost-effective p-type semiconductor (Chakravarty et al., 2015) with a narrow band gap of about 1.2eV (Dar, Nam & Kim, 2010). It has been widely used particularly for environmental treatment

because of its unique properties. Moreover, cobalt nanopartilce has emerged as novel nanocatalyst for azo dye degradation.

Several new routes have been developed for the synthesis of transition metal oxide nanoparticles such as hydrothermal, sol gel (Glaspell et al., 2005), mircoemulsion, microwave assisted synthesis (Ong et al., 2016) and so on but few are reported with controllable size and shape of the nanoparticles as rapid surface oxidation is the key issue in CuO synthesis. For this, one might have to use some capping agent/surfactants for example, Cetyl trimethylammonium Bromide (CTAB) (Wu & Chen, 2004), Sodium dodecyl sulphate (SDS), Poly ethylene glycol (PEG) (Wang et al., 2002), carboxylic acid, oleic acid, and Poly vinyl Pyrolidine (PVP) (Deng et al., 2013) to prevent aggregation and oxidation.

In 2013, Zhu and co-workers successfully synthesized CuO nanosheets *via* hydrothermal method in the presence of CTAB as capping agent and tested for oxidative degradation of Methylene Blue (MB) with H_2O_2 as green oxidant. They concluded that CuO nanosheets show high catalytic activity as complete degradation of MB was observed in total reaction time of 180 minutes. However, they found their catalyst stable and reusable in three successive cycles.

In another study, cupric oxide was fabricated with different morphologies (plate-like, Flower-like and boat-like) through hydrothermal synthesis by simple variation of reaction conditions in the presence of Polyethylene Glycol (PEG) as stabilizing agent. The catalytic activity was explained against the oxidative degradation of Methylene Blue (MB) in the presence of H_2O_2. Results showed no degradation without H_2O_2 and almost 20% decolorization in the absence of CuO catalyst after 15 hours. When both catalyst and oxidant were added in the reaction mixture, degree of degradation increased and reached up to 97.2%, 96.0% and 96.1% with plate-like, flower-like and boat-like respectively, in 10 hours (Yand & He, 2011).

A new and facile study was conducted to evaluate the catalytic activity of hollow cobalt nanoparticles for the rapid and efficient reductive degradation of four azo dyes namely;

Methyl Orange (MO) and Congo Red (CR), Orange G and amaranth. The cobalt nanoparticles were synthesized by a galvanic replacement reaction in which Al (aluminium) nanoparticles were used as templating agent. The results showed complete reduction of MO in 90 minutes while slow degradation was observed for other three dyes following the order: amaranth> orange G> congo red (Sha et al., 2016).

Recently in 2016, a study was reported by Bhattacharjee and Ahmaruzzaman in which CuO nanorods and CuO nanosheets were fabricated *via* microwave assisted green synthesis process in the presence of amino acids as stabilizing agent. The catalytic activity of as prepared nanostructures was tested for reduction of 4-nitrophenol into 4-aminophenol. They also checked photocatalytic degradation of MB and Eosin Y. By comparing the results of nanorods and nanosheets, it was concluded that 1D CuO nanorods serve more efficiently for the catalytic reduction as it completely reduced 4-Np into 4-AP in 8 min while 2D nanosheets complete the same reaction in 14 min of reaction time. On the other hand, for the degradation of dye, 2D nanosheets are proved to be more active (Bhattacharjee & Ahmeruzzaman, 2016).

In the present study, CuO nanoparticles were synthesized *via* chemical reduction method in the presence of Polyethylene Glycol as capping agent and sodium borohydride as reducing agent. The above synthesis method was chosen because it is economically feasible, energy efficient, high throughput and can be easily scaled up on the industrial scale. The selected synthesis method was slightly modified by using water as solvent in the reaction medium instead of organic solvent (ethanol). The catalytic activity of prepared nanoparticles was tested for oxidative and reductive degradation of organic dyes (MB and MO) and 4-nitrophenol.

It is well known, extremely small size and high surface area are important factors for the spectacular catalytic reactivity of metal nanoparticles (Cao et al., 2016). However, it is crucial to maintain the effective surface area because pure metal nanoparticles can easily be aggregated in the aqueous medium which would seriously weaken their catalytic activity during the catalytic reactions. Considering this problem,

immobilization/Stabilization of metal oxide nanoparticles (NPs) onto certain inert supports such as alumina, silica or graphene is adopted as an ideal strategy that provides a heterogeneous catalyst system to stabilize the catalyst surface area and prevent aggregation (Vartooni et al., 2015). Moreover, it is highly preferable to use a heterogeneous catalyst system because of its acquiescence with the principles of green chemistry; proposing low energy synthesis procedure of nanocomposites, avoiding the use of ancillary species and facilitate the catalyst recovery to reuse, thus minimizing the waste generation after the completion of catalytic reaction (Parlett, et al., 2013).

A comparative study was conducted by Zhou and co-workers in 2013 to show the positive effect of supported nanocomposite with enhanced catalytic activity. They synthesized Cellulose Nanocrystals (CN) supported CuO nanoparticles and evaluated for catalytic reduction of 4-Nitrophenol into 4-aminophenol in the presence of $NaBH_4$. Later on, catalytic activity of CN supported CuO NPs was compared with the unsupported CuO NPs. It is revealed in their research that conversion rate of CN supported CuO nanohybrid reached upto 100% in 60 sec as compare to the unsupported CuO NPs that was 68% with the same reaction conditions. Both results indicate that the higher catalyzed reaction might be associated with the large surface area of CN supported CuO NPs which may decrease due to the agglomeration of unsupported CuO NPs in the aqueous media (Zhou et al., 2013).

Chong et al., 2016 reported magnetic Fe°/Fe_2O_3/graphene nanocomposite for the rapid degradation of three organic dyes namely; Methylene Blue (MB), Methyl Orange (MO) and Crystal Violet (CV). The nanocomposite was successfully synthesized by single step reduction method using NaBH4 as reducing agent. The results showed that Fe nanocrsytals dispersed efficiently in the interlayer of graphene nanosheet which could increase the active surface sites for the adsorption and reductive degradation of dyes. After 20 min of reaction time, the decolorizaion rate of MO, MB and CV were 94.78%, 91.60% and 89.0% respectively. In addition, they suggested that the prepared Fe°/Fe_2O_3/graphene nanocomposite exhibited ferromagnetic properties which could be easily separated and reused.

1.3. γ- alumina as a support for nanocatalysts

With growing attention on environmental remediation and sustainable development, it is preferable to use renewable natural materials for catalyst deposition. Among the various nanomaterials, use of alumina as catalyst and catalyst support is of great interest because of its presence and significance in natural aquatic environment (Horden, 2004). Alumina nanoparticles or alumina nanocomposites have found valuable applications in drinking and wastewater treatment due to their distinct properties such as low cost, high surface area, good mechanical strength and enhanced thermal stability (Karim et al., 2011; Sharma et al., 2008). Among the transition aluminas (which are heated at temperature below 1100 °C), gamma alumina (γ-Al_2O_3) is most important active alumina studied widely as catalyst and catalyst support.

Several methods have been developed for γ-Alumina synthesis as thermal stability is the key issue to obtain the desired product. Each type or structure of alumina formed depends on the starting or precursor material and its temperature range of existence.

$$\text{Boehmite (AlOOH)} \xrightarrow{450\ ^\circ C} \gamma\text{-}Al_2O_3 \xrightarrow{600\ ^\circ C} \delta\text{-}Al_2O_3 \xrightarrow{1050\ ^\circ C} \theta\text{-}Al_2O_3 \xrightarrow{1200\ ^\circ C} \alpha\text{-}Al_2O_3$$

γ-alumina is classified as low temperature alumina ($Al_2O_3.nH_2O$) formed by thermal dehydration (calcination) of precursor boehmite/aluminium oxide hydroxide (AlOOH) at temperature below 600 °C, calcination above this temperature leads to the formation of other metastable alumina such as δ, θ, and α- alumina, called as high temperature aluminas. In term of catalytic activity, low temperature alumina are more active because of high surface area and more surface active sites are available as compared to the high temperature alumina where proton transfer readily takes place on the surface and results in the gradual loss of surface area (Horden, 2004).

γ- Alumina structure

As γ-Alumina is synthesized at temperature below 600 °C so its structure is traditionally considered as a cubic defect spinal type where oxygen lattice is assembled by a cubic close-packed stacking of oxygen layers with Al atoms occupying the octahedral and

tetrahedral sites. In the defect spinal structure, trivalent Al cations are responsible for defective nature which creates a portion of 'non spinal' sites where lattice position remains vacant in the ideal spinal structure (Trueba & Trasatti, 2005).

Recently, many attempts have been made to synthesize γ-Alumina with a defined pore volume and surface area preserved after calcination at high temperature where surfactants or non-surfactants are used to maintain the structural directing properties. In addition, most of the γ- aluminas are impregnated with the transition metal precursors such as (Cu, Co and Ni) in aqueous solution that maintain their thermal stability in terms of high surface area or pore volume, thus greatly improving their usefulness in the catalysis applications including catalytic degradation of organic compounds. Moreover, dispersion of transition metal oxides on the surface of alumina inhibits the transformation of γ-Alumina into α-alumina at high calcination temperature, thus maintaining the high catalytic activity of γ-Alumina by preserving its high surface area.

Numerous studies have been reported to disperse transition metal oxide nanoparticles on γ-Alumina such as sol gel method (Sogand et al., 2013), hydrothermal synthesis and homogenous deposition precipitation method and ion adsorption method.

Ndolomingo and co-workers synthesized γ-Alumina supported copper oxide nanocatalyst *via* homogenous deposition precipitation method. The catalytic activity of as prepared nanocomposite was evaluated to study the kinetics of the catalytic oxidation of organic dye (Methylene Blue) with H_2O_2 under ambient conditions. They found alumina based copper oxide nanocatalyst very active in the oxidation of MB as 80% degradation was observed in 120 minutes and almost no degradation was observed in the presence of H_2O_2 without catalyst even after 120 minutes (Ndolomingo & Meijboom, 2015).

According to Hua et al, Catalytic Wet Air Oxidation (CWAO) is a useful technique to deal with most of the organic azo dyes. CuO/γ-alumina nanocomposite was synthesized by consecutive impregnation method and evaluated for CWAO of three azo dyes which were Methyl Orange (MO), Direct Brown (DB) and Direct Green (DG). The results indicated 90% removal of dyes in very short reaction time of 90 minutes at high

temperature. According to the results, hydroxyl radicals were responsible for the azo bond and benzene ring fragmentation and as a result desulfulration occurred with the decolorization thus, oxidizing the dye molecule into final oxidation products such as water and carbon dioxide (Hua, Ma & Zhang, 2013).

Herein, we used commercially available γ-Alumina as a support for metal oxide nanoparticles. Copper oxide and cobalt oxide nanoparticles were successfully deposited onto γ-Alumina *via* homogenous deposition precipitation (HDP) method. In this method, metal precursors are easily precipitated on a support by a controlled increase in temperature and pH by adding urea in the reaction mixture which gives highly loaded and well dispersed metal nanoparticles on the support (Din et al., 2014). Later on, the as synthesized and characterized nanocatalysts are evaluated to accelerate the degradation of organic dyes namely; Methylene Blue (MB), Methyl Orange (MO) and other organic pollutant such as 4-Nitrophenol (4-NP) from the industrial wastewater streams.

1.4. Significance of Study

Our reported research will explore new, environmental friendly and cost effective nanocatalysts that offer a viable alternative, as compared to the expensive noble metals that will show excellent catalytic activity for oxidative and reductive degradation of organic pollutants in aqueous medium. To the best of our knowledge, fewer studies have been reported on the fabrication of γ-alumina supported transition metal oxide nanoparticles for wastewater treatment so far. Our designed research will be helpful to open a novel and perceptive way to modify the heterogeneous catalyst system for industrial scale removal of organic pollutants.

1.5. Aims/objectives

To meet the growing needs of society within the limited water and energy resources in an efficient and reliable way, research is carried out for the wastewater treatment with the development of new nanocatalysts having advanced properties.

Hence, the objectives to design and carrying out this research were to;

- Synthesis of nanocatalysts by different methods
- Characterization of selected nanocatalyst by using different analytical techniques, (XRD, TGA and SEM)
- Application of selected nanocatalysts for the removal of selected organic contaminants from simulated wastewater
- Catalyst efficiency will be determined towards the removal of organic pollutants

CHAPTER # 2

MTERIALS AND METHODS

MATERIALS AND METHODS

The research work was carried out at Nanoscience and Technology Division (NS & TD), National Centre for Physics (NCP), Quaid-i-Azam University (QAU) campus, Islamabad.

2.1. Materials

All chemicals were of analytical grade and used without further purification.

γ-alumina (γ-Al_2O_3) Copper Nitrate. trihydrate [Cu $(NO_3)_2.3H_2O$], Cobalt Nitrate Hexahydrate [Co_2 (NO_3). $6H_2O$], Urea [CO $(NH_2)_2$], Ammonia Solution (NH_4OH), Sodium borohydride ($NaBH_4$), Hydrazine Hydrate (N_2H_4), Methylene blue ($C_{16}H_{18}N_3SCl$), Methyl Orange ($C_{14}H_{14}N_3NaO_3S$), 4-Nitrophenol ($C_6H_5NO_3$), Polyethylene glycol (PEG,4000), Ethanol (C_2H_5OH), Acetone (C_3H_6O), Hydrogen Peroxide (H_2O_2, 30%) were purchased from Sigma Aldrich. De-ionized water was used as solvent in all experimental procedures.

2.2. Synthesis procedures for nanoctalysts

2.2.1. Synthesis of Copper nanoparticles

2.2.1.1. Microwave assisted method

Initially, copper oxide nanoparticles were synthesized *via* microwave assisted method. Typically, the synthesis procedure started with the mixing of 1g of Cu $(NO_3)_2.3H_2O$ in 25 ml of ethanol. In a separate beaker, another ethanolic solution was prepared with 0.5 g of polyethylene glycol (PEG) containing a pellet of sodium hydroxide to maintain the pH of the solution. Two fractions were then mixed together in a 50 ml round bottom flask. This resulted in a color change of solution from light to dark blue. The reaction solution was then placed inside a conventional microwave oven after adding 100 µl of Hydrazine hydrate as reducing agent to heat the mixture in 3 cycles (10 sec on, 10 sec off and stirring). Upon heating, solution changed from blue to deep brown indicating the formation of copper oxide nanoparticles (Wang et al., 2002). This resulted in the formation of mixed copper oxide NPs (Cu_2O, CuO) due to the improper heating and stirring in domestic microwave oven, while the desired product was only CuO NPs.

After that, we successfully synthesized pure CuO NPs *via* chemical reduction method (Wang et al, 2004). The procedure was modified to meet the principles of green chemistry where de-ionized water was used as solvent and reaction solution was set on conventional heating equipped with magnetic stirrer that ensured the homogenous mixing of reactants to create desired product.

2.2.1.2. Chemical reduction method

In a typical procedure, reaction mixture was prepared in two separate beakers containing 25ml of de-ionized water each. 1g of Cu $(NO_3)_2.3H_2O$ was mixed in one beaker and the other having 0.5g of Polyethylene glycol (PEG). Two fractions were then mixed together in a 100ml beaker and pH was adjusted as 10 by adding ammonia solution dropwise in the reaction mixture. This resulted in a color change of solution from light blue to dark blue due to the formation of copper ammonia complex. After that, the resulting solution was reduced using 25mg of $NaBH_4$ at 60 °C. Solution immediately changed to deep brown color indicating the formation of copper oxide nanoparticles. Precipitates were obtained after centrifugation of solution at 5500rpm for 20 min. Supernatant was decanted and the residues were washed with water to remove any water-soluble impurity. The process was repeated again with methanol and acetone to remove organic impurities. It was then dried in vacuum oven at 80°C for 3 hours and collected. (Wu and Chen., 2002)

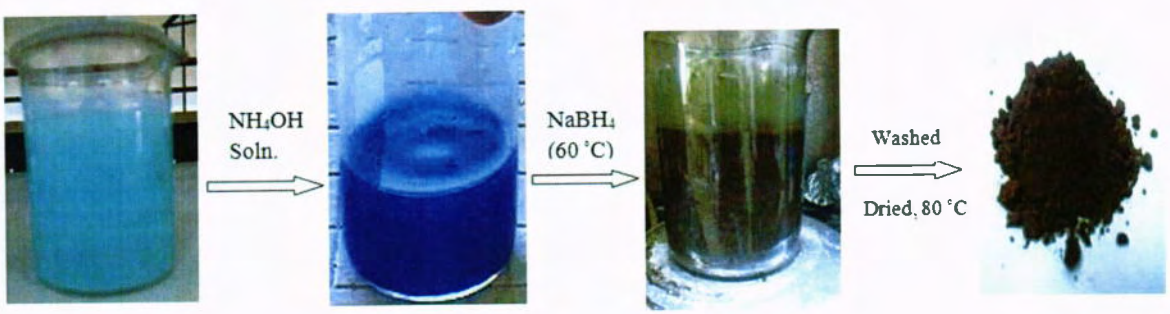

Figure. 2.1. Step by step synthesis of copper nanoparticles.

2.2.2. Synthesis of γ-Alumina supported copper nanocatalysts

With growing attention on environmental remediation and sustainable development, it is preferable to use renewable natural materials for catalyst deposition. Among the various nanomaterials, use of alumina as catalyst support is of great interest because of its presence and significance in natural aquatic environment (Horden, 2004).

In the current research, commercially available γ-alumina powder was used as a support for the dispersion of copper oxide nanoparticles via homogenous deposition precipitation method. A typical synthesis route for Cu/Al_2O_4 nanocomposite is as follows: 0.5g of γ - alumina and 0.025g of precursor salt [Cu $(NO_3)_2.H_2O$] were mixed in 50ml of de-ionized water and kept on continuous stirring overnight at room temperature, which resulted in the formation of light blue color solution. Then, 0.02g of urea was added as a precipitating agent and resulting solution was maintained at 80°C for 2 hours to decompose urea. Thermal decomposition of urea slowly generates in situ ammonia and hydroxyl ions in the solution that gradually increases pH from neutral to basic which ensured the slow precipitation of metal oxide in the support porosity. In basic medium and at low temperature such as 60-80 °C, metal hydroxide Cu $(OH)_2$ thermally decomposed into CuO in aqueous solution. (Alini et al 2005).

The mixture was then cooled and reduced by adding 0.04g of $NaBH_4$ under vigorous stirring, resulted in an immediate color change from light blue to brown indicating the formation of CuO nanoparticles onto γ-alumina . The resulting solution was allowed to stir for 2 hours to complete the reaction. Precipitates were filtered and washed with de-ionized water to remove any impurity and then dried overnight in vacuum oven at 80°C. Dried product was finely crushed (grounded/grind) and saved for further use (Ndolomingo et al., 2015).

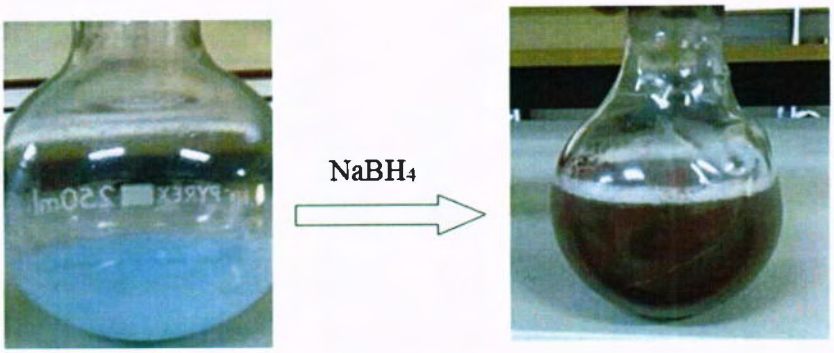

Figure.2.2. Synthesis of γ-Alumina supported copper nanocatalysts

2.2.3. Synthesis of γ-Alumina supported cobalt nanocatalysts

Commercially available γ-alumina powder was used as a support. γ -alumina supported cobalt nanocatalysts were synthesized *via* homogenous deposition precipitation method. In a typical experiment, 0.5g of γ -alumina and 0.025g of cobalt nitrate hexahydrate [$Co(NO_3)_2.6H_2O$] were mixed in 50ml of de-ionzed water and kept on continuous stirring overnight at room temperature. Then, 0.02g of urea was added as precipitating agent and maintained at 80°C for 2 hours. After that, the reaction mixture was cooled and 0.04g of sodium borohydride was added under vigorous stirring. Finally, resulting solution was maintained for 2 hours at room temperature. The resulting white precipitates were harvested through filtration and washed with de-ionized water to remove any soluble impurity and then dried overnight in vacuum oven at 80°C. Dried product was crushed into fine powder before use (Ndolomingo et al., 2015).

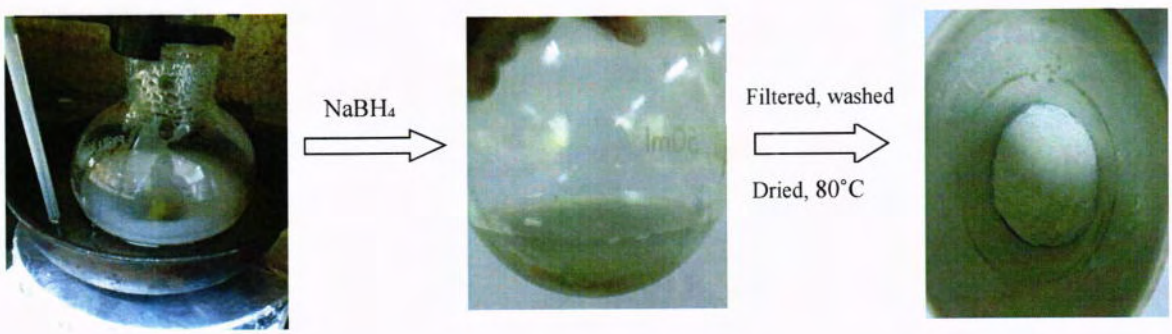

Figure 2.3. Schematic illustration of γ-Alumina supported cobalt nanocatalysts

2.3. Catalyst characterization

The as synthesized nanocomposites were characterized using a series of analytical techniques such as X-Ray Diffraction (XRD), Scanning Electron Microscopy (SEM) and Thermogravimetric Analysis (TGA). UV/ visible spectroscopy was used to record the absorption spectra and to monitor the extent of percent degradation. A brief understanding to these techniques is summarized below:

2.3.1. UV/ visible spectroscopy

In the present study, liquid samples were analyzed in LAMBDA 25 UV/vis spectrophotometer, Perkin Elmer using standard rectangular quartz cuvette of 10cm path length and 3ml volume.

2.3.1.1. Introduction

UV/visible spectroscopy is the simplest analytical technique, used to study the response of a chemical towards UV/visible light. It covers about 200-400nm (UV) and 400 – 800nm (visible) region of the electromagnetic spectrum. It is used to study the absorbance in term of wavelength and determine the concentration of an unknown sample through which the rates of reactions and equations for reaction mechanisms can be proposed.

2.3.1.2. Basic principle behind the sample analysis

When a beam of light interacts with a sample, some of the light may be absorbed and the remainder transmitted through the sample (Meyers, 2000). Chemicals in the sample absorb electromagnetic radiations, but only of specific energy. The absorbed photons of the UV and visible light by the molecule (or atom) increases the energy content of the molecule which produces electronic transitions in different energy levels. These electronic transitions occur as a result of excitation of outer electron from lower energy level (ground state) to higher energy level (excited state). This creates a very narrow absorbance band at the particular wavelength known as **lambda max** (λmax), shows maximum absorbance of the absorbing species in the sample. Most of the absorption of organic compound is based on the n $\rightarrow$ π^* and π $\rightarrow$ π^* transitions because absorption band of these transitions fall in the region of UV/visible spectrum (200 - 700nm). Thus, it is important for a molecule to be characterized by the UV/visible spectroscopy to have unsaturated group to provide π electrons (Zhang, 2007). The same effect occurs when group containing n electron are conjugated with π electron groups.

2.3.1.3. Absorbance and transmittance

When a beam of light passes through or reflected from the sample, it is recorded as the ratio of the intensity of the light as incident radiation *(I_o)* to the transmitted radiation *(I_t)* by the sample at the particular wavelength, called as transmittance (T). It is usually represented as percent transmittance (% T) or in term of a fraction of 1.

$$\% T = (I/I_o) * 100$$

Absorbance (A) is usually expressed as negative log of transmittance:

$$A = - \log T \text{ or } -\log (I/I_o)$$

Beer - Lambert law

The most important principle behind the absorption analysis in UV/visible spectroscopy is the Beer Lambert law and it is strictly followed only for monochromatic radiations.

$$A = \varepsilon cl$$

A= Absorbance, ε = molar absorptivity of the sample, c = concentration (mol/l), l = path length (cm).

The above equation is the combination of two laws which states that absorbance of radiation is directly proportional to the concentration of absorbing molecule in a sample (Beer's law) and second is the absorbance is related to the path length. (Lambert'law). This law specifically holds only for low concentrations. At higher concentrations, absorbing molecule mutually interact with each other (aggregation, dissociation) and with the solvent. In this case, "ε" is not independent of concentration "c". For the upper concentration limit (concentrated samples), a calibration curve has to be used rather than straight calibration line (Liauw et al., 2010).

2.3.1.4. Absorption spectrum of organic dyes

As is well known, most of the organic compounds show absorption spectra due to the presence of (unsaturated) π electrons so the functional groups such as chromophore and

auxochrome affect the λ_{max} in the UV/visible region. Chromophores are basically the color bearing group in the dye molecule that provide π electrons which produces absorption between 185-1000nm. Commonly used chromophores are nitro (-NO_2), azo (-N=N-) and carbonyl (C=O) groups while the color of the molecule may be intensified by the auxochrome to which it is attached. The most important auxochromes are OH, NH_2, CH_3 and NO_2. Position of the absorption band at the particular wavelength determines the presence of the specific choromophore in the molecule. However, λ_{max} is affected by the parameters such as choice of solvent, pH and temperature in terms of wavelength shift and peak intensity.

2.3.1.5. Instrumentation

A schematic diagram of UV/visible spectrophotometer is shown below. Analysis starts with a light source (a combination of tungsten/halogen and deuterium lamp) to generate UV and visible radiations covering 200-800nm. The beam of the light is focused onto diffraction grating that splits the light into its component color of different wavelengths just like a very efficient prim.

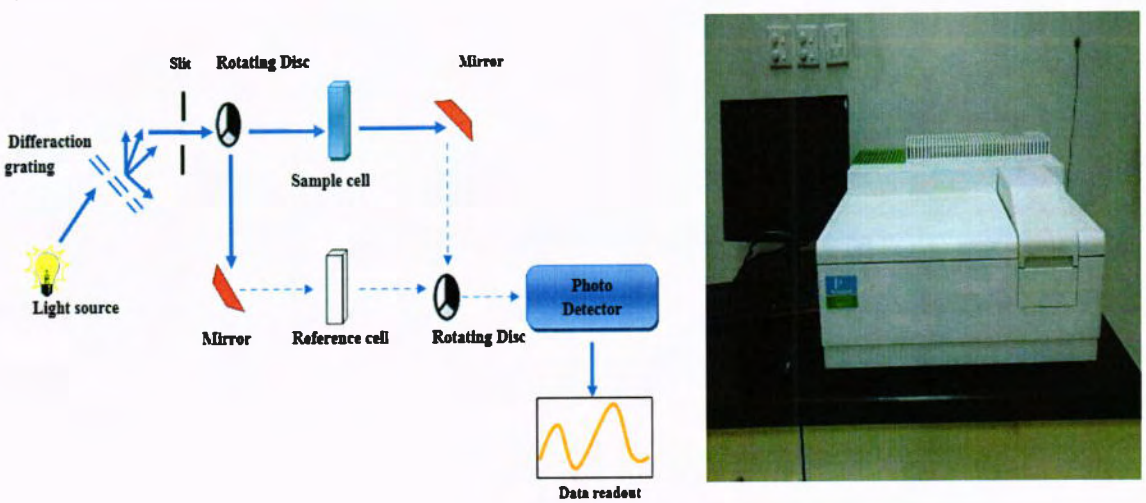

Figure 2.4. Schematic Diagram of UV/vis Spectroscopy and picture of UV/vis spectroscopic instrument.

Typically, when the light beam passes through the liquid sample which is placed inside the vertical, transparent container called cell or cuvette (The reference cell or cuvette

contains the solvent in which sample is dissolved known as **blank).** It takes approximately 30 sec to scan the sample, and then the radiation of the same wavelength passes through the reference cell. Photo detector converts the light into tiny electric currents and absorption spectrum is generated by comparing the intensity of the light passing through the sample cell (I) and reference cell (I_o) and absorbance is related to the following equation.

$$A = -\log (I/I_o)$$

Ideally, A=1 which indicates the 90% light absorbed by the sample. The higher the current, the greater the intensity of the light. The data readout plots the spectrum of intensity against wavelength (nm).

2.3.2. X-ray diffraction spectroscopy

The functionality of the nanomaterials is defined by their crystalline structure which leads to extraordinary change in nanoparticle properties. (Moreau et al 2013). In the current study, crystal structure of dried and fine grained nanopowder is investigated by X-ray diffraction (XRD) diffractometer (Bruker D8 Advance diffractometer) at room temperature using CuKα radiations over a 2θ range of 10°–80°.

2.3.2.1. Introduction

XRD is the one of the sophisticated and non-destructive characterization techniques to identify the chemical compounds from their crystalline structure, not from their chemical compositions. It helps to provide information about crystallite size, orientation of crystal structure and phase composition of semi crystalline polymers.

2.3.2.2. Bragg's Law/Basic principle

In general, X-rays are high energy electromagnetic waves of shorter wavelength in the order of 0.1 nm. The basic phenomena behind the X-ray diffraction methods is wave interferences which may be constructive interference (in phase) when phase difference is of nλ (n is an integer), or may be destructive interference (completely out of phase) when

phase difference is of nλ/2 because two light waves of same wavelength and travelling in the same direction can either reinforce or cancel each other, depending on their phase differences. The basic principle by which the diffraction occurs is based on Bragg's Law which states that path difference between two X-ray beams depends on the incident angle (θ) and spacing between the parallel crystal planes (d).

$$n\lambda = 2d \sin \theta$$

According to the equation, constructive interference (in phase) is only created when path difference is equal to one or multiple of x-ray wavelength (nλ).

- Knowing the information about the spacing between the atomic planes, one can determine the crystal structure.
- Miller indices (hkl) represent the crystallographic planes of a crystal. When the algebraic sum ($h^2+k^2+l^2$) is equal to 1, the plane index will be (001) and if it is equal to 2, it should be (110). These are the series of parallel line in the crystal structure with the spacing d_{hkl}.

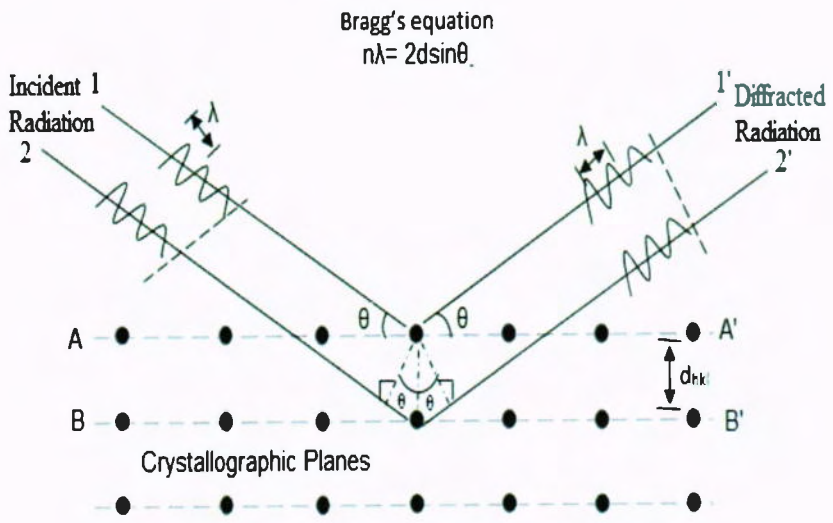

Reprinted from Leng, Y. (2008). Material characterization: Introduction to microscopic and spectroscopic methods. Clementy loop, Singapore. John Wiley & Sons

2.3.2.3. Instrumentation/X-ray differactometer

The XRD instrument is called an X-ray diffractometer. The basic function of a diffractometer is to detect X-ray diffraction from materials and to record the diffraction intensity as a function of the diffraction angle (2θ). Every crystalline solid is characterized by its distinctive X-ray powder pattern which may be used as a fingerprint for its detection. The X-ray radiation is emitted by an X-ray tube that passes through special slits which collimate the X-ray beam. These slits are made from a set of closely spaced thin metal plates parallel to the figure plane to prevent beam divergence in the direction perpendicular to the figure plane. A divergent X-ray beam passing through the slits strikes the specimen. The specimen is usually in the form of a thin plate in a round shaped sample holder. X-rays are diffracted by the specimen and form a convergent beam at receiving slits before they enter a detector. The diffracted X-ray beam passes through the monochromatic filter (or a monochromator) before being received by a detector.

Commonly, the monochromatic filter is placed in the diffracted beam path instead of the incident beam path. This arrangement can suppress wavelengths other than Kα radiation and also decrease background radiation originating within the specimen. (Kα X-rays are emitted when K shell vacancies are filled by electron of either L or M shell. Kα1 and Kα2 radiations with the small wavelength difference (0.15406nm and 0.15444nm) are usually combined and called as Kα doublet.) Kα doublet generated by a copper target is the most commonly used monochromatic X-ray in diffraction mechanism because of its shorter wavelength, based on Bragg's Law.

2.3.2.4. Diffraction Peak and Phase Identification

A diffraction peak is generated at the Bragg angle θ_B satisfying the Bragg conditions. For the crystalline structure and crystalline phase identification, Powder diffraction files (PDF) have been published by the International Centre for Diffraction Data (ICDD) which is updated and expanded from time to time. Crystal structure and phase is determined by analyzing, then comparing the spectrum with a PDF containing over 60,000 diffraction spectra of known crystalline substances (Yeng, 2008).

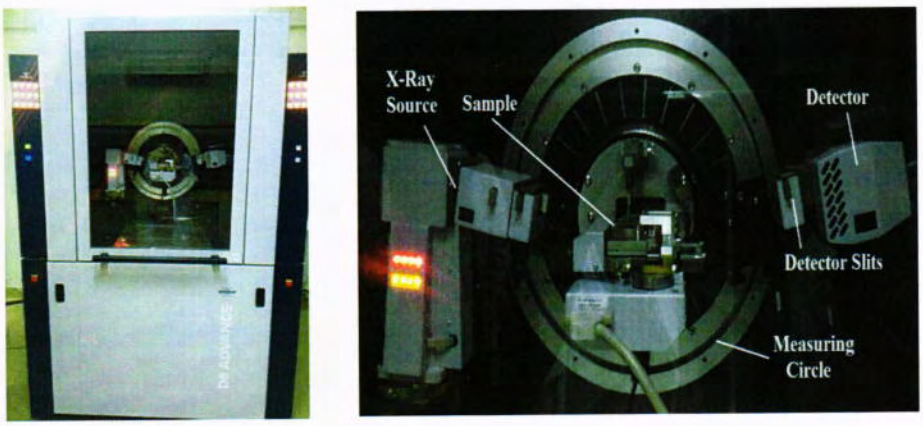

Figure 2.5. Pictures of XRD instrument at NCP.

2.2.3. Scanning Electron Microscopy (SEM)

2.2.3.1. Introduction

The scanning electron microscopy (SEM) is a type of electron microscopy, used to magnify the microscopic structure of a particular object by scanning the surface of object with high energy beam of electron. It is a non-destructive technique, provides with a three dimensional image with a much higher resolution up to *300000 as compare to the conventional light microscope up to~10000 but as the images are not produced by the light waves, these are black and white in appearance. An important feature is that, it is highly sensitive to the even small variation in surface composition that provides useful information about surface morphology and the distribution of metal nanocatalysts on the support. Moreover, it provides valuable information about the purity of the sample as well as the extent of agglomeration (Herrera & Sakulchaicharoen, 2009).

2.3.3.2. Instrumentation/Signal detection

In SEM, electrons are produced by an electron gun. When electrons strike the atoms of the specimen, numerous complex events take place in the form of signals. Secondary electrons back scatter electrons and characteristic X-rays are generated that yield the information about the specimen topography and composition. Image of the specimen can be constructed on every point by having the appropriate detector. For example, SEM can produce three-dimensional and high resolution image of 1-5nm in size with the electrons arising from the primary detection mode i.e. secondary electrons imaging. Secondary

electrons are produced by inelastic scattering and ejected from the atom of the specimen. A second image is produced by the characteristic X-ray which results from the ejection of inner shell electrons of the specimen and these are used to identify the elemental composition of the specimen by a technique called Energy Dispersive X-ray (EDX). Backscattered electron image provides information about the composition beneath the sample. It is affected by the atomic number because these signals result when original beam electrons are elastically scattered from the atomic nuclei within the substrate.

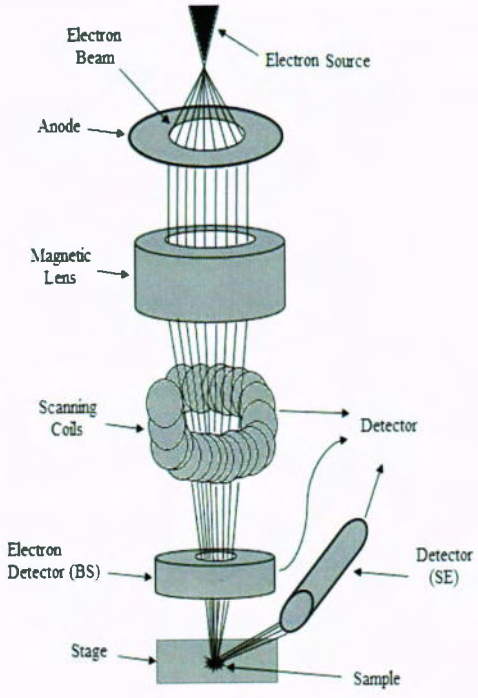

Figure 2.6. Schematic diagram of SEM

In a typical SEM, the beam passes through the deflection system or the pair of electromagnetic coils (scanning coils) in the electron column and then to the final lenses such a condenser lens and one objective lens. These lenses are important for electron probe formation and deflect the electron beam horizontally and vertically which scans the specimen in a raster fashion over rectangular area. The signals emitted from the specimen are recorded by a detector, amplified and displayed on Cathode Ray Tube (CRT) or liquid Crystal Display. The image displayed are digitized and in the form of distribution map which shows the intensity of the signal generated by the scanned area of the specimen (Leng, 2008 and Joshi, 2008).

2.3.4. Thermogravimetric Analysis (TGA)

During the current research project, TGA of as obtained nanocatalyst was carried out on TGA/DSC simultaneous thermal analyzer (Model STARe system)/METTLER-TOLEDO was used from the ambient temperature to 800 °C with the heating rate of 10 °C/min under air flow using 5.9 mg of sample.

2.3.4.1. Introduction

Thermogravimetric analysis (TGA), or simply thermogravimetry (TG), is a technique for measuring the mass changes in the sample that occurs as a function of temperature overtime in accordance with a controlled temperature program, T (t) in a controlled atmosphere. The program can be either isothermal, or non-isothermal. In the most common non-isothermal program, temperature changes linearly with time so that the heating rate is constant. A typical temperature range of TGA is from ambient to 1000-1600 °C. Controlled atmosphere is created by the nature of the purge gas which may be inert (nitrogen, helium or argon) or oxidizing (air, or oxygen) or reducing (8-10% hydrogen or nitrogen). Controlled atmosphere can be dynamic or static. In dynamic atmosphere, purged gas runs around the sample at a certain flow rate (50-100ml/min while in controlled static atmosphere; pressure of the gas can be reduced as low as 10^{-3}-10^{-4} pa.

2.3.4.2. Mass change studies

The samples studied by the instrument are either solids or low volatility liquids ranging in size from 1-100mg. Mass changes measurement by TGA may be categorized as loss or gain in mass when sample is heated or cooled. Mass loss processes include: degradation and/or decomposition resulting from bond breakage of compound at about 200 °C but not more than 800 °C, vaporization of volatile liquids (between ambient and 300 °C), evaporation of water content at 100 °C, reduction of metal oxide into metals and desorption of gases. A mass gain can be observed as a result of adsorption of gases and reaction of solids with reactive gases. In general, all these mass changes are determined

by TGA to extract information about the sample composition, extent of cure and thermal stability (Prime et al., 2009).

2.3.4.3. Basic principle and instrumentation

The heart of the modern TGA lies in the thermobalance (balance and a furnace), both of which are controlled electronically and measure the sample mass as a function of temperature and time. The arrangement pattern between the furnace and balance differ from one instrument to another. Position of the furnace can either be vertical or horizontal with respect to the sample, in either case sample is held in two ways. It may be hanged down off or supported on the balance beam. The sample holder is rigidly attached to the end of the balance beam. Both sample and furnace are enclosed in an airtight compartment made of glass, fused silica or metal. A gas or gases are injected through an inlet port. However, most of the samples are analyzed in inert atmosphere that carries away the decomposed gaseous products and protect the thermobalance from condensation and corrosion. The mixture of the inert gas and the product leave the instrument through an outlet valve. In vertical arrangement, nitrogen gas in replaced by the heavier inert gas such as argon in order to avoid the flow of degradation products towards the balance mechanism.

Furnace temperature and sample temperature is monitored by the thermocouple, placed closed to the proximity of the furnace and sample. Ideally, furnace temperature must be identical to the sample temperature.

Arrangement of Thermobalance

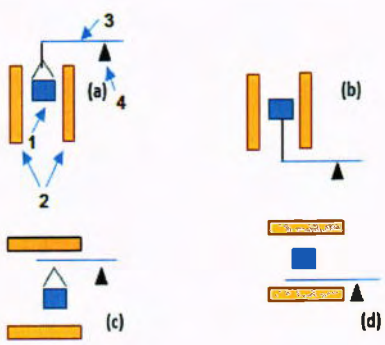

(a) Vertical suspended
1. Sample holder 2. Furnace
3. Balance beam 4. Fulcrum
(b) Vertical supported
(c) Horizontal suspended
(d) Horizontal supported.

Instrumentation

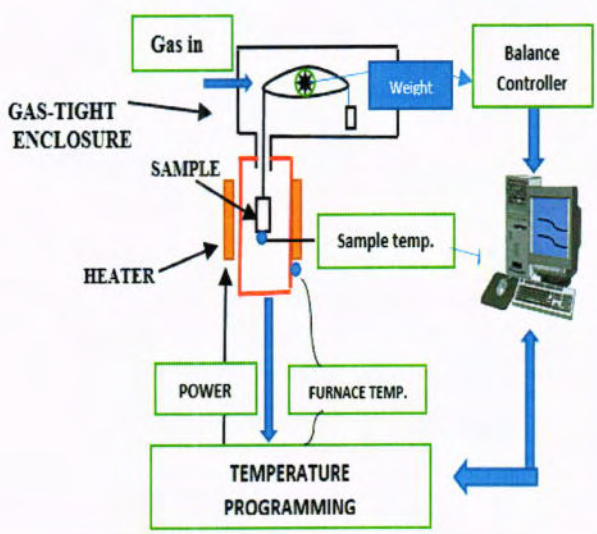

Figure 2.7. Schematic arrangement of thermobalance in TGA and its instrumentation.

Themogravimetric curve is represented as a result of TGA. It may be in integral (TG curve) or differential (DTG curve) form. In TG curve, mass is plotted against time or temperature while DTG curve is the derivative of TG curve and plotted as time against temperature (Vyazovkin, 2012).

2.4. Catalytic experiment

During recent years, a great deal of research has been focused on fabricating the nanomaterials that have potential catalytic applications in wastewater treatment. In this study, to evaluate the superior activity of our as prepared nanoparticles (CuO, Cu/Al_2O_4 and Co/Al_2O_4) as efficient and active catalysts, we demonstrate the catalytic activity towards the oxidation and reduction degradation of organic dyes namely Methylene Blue (MB), Methyl Orange (MO) and also 4-NP as model system.

The progress of catalytic reaction was monitored using UV/vis spectrophotometer by taking small aliquots of experimental solution in standard quartz cuvette of 1cm path length and 3ml volume. After UV/vis analysis, reaction solutions were transferred back to the beaker and were continuously stirred using magnetic stirrer to ensure the homogenous mixing of reactants and distribution of catalyst. UV/vis spectra were recorded at different time intervals (0, 8, 15, 30 and 45 minute) to evaluate the contact time as reactions proceed. The absorption spectrum recorded just after the preparation of experimental solution was considered as "0" minute spectra. The extent of catalytic activity was confirmed by the decrease in the peak absorbance of the contaminant with time. As a result, optical absorption spectra were plotted against wavelength.

Blank reactions were recorded by preparing the reaction solution without catalyst while all the other parameters were kept constant in order to show that the reaction does not proceed in the absence of catalysts. Moreover, the effects of various experimental parameters such as temperature, H_2O_2, $NaBH_4$ amount were also investigated to check the time dependent activity of catalyst for degradation.

2.4.1. Catalytic degradation of organic dyes

For measuring dye degradation activity of catalysts, we have selected Methylene Blue (MB), Methyl Orange (MO) as model reaction. In this process, dye stock solution of concentration 0.5mM was prepared by dissolving 15mg of powder dye in 100ml of de-ionized water. The desired reaction solution of dye concentration 0.06mM was obtained by appropriate dilution of respective stock solution. For this, 1.2ml of stock solution of MB and MO was diluted by adding 8.8ml of de-ionized water. Immediately to dye solution, 10mg of catalyst was added. For oxidative degradation, 2.5ml of H2O2 was used as a green oxidant and 1 ml of NaBH4 was added for reductive degradation in reaction mixtures.

Concentration of MB and MO were monitored at 665 and 464nm respectively.

2.4.2. Catalytic reduction of 4-NP

For the reduction of 4-nitrophenol into 4-aminophenol, Stock solution of concentration 0.9mM was prepared by dissolving 12mg of 4-nitrophenol in 100ml of water.

Experimental solution was obtained by appropriate dilution up to concentration of 0.1mM by taking 1.1ml of stock solution in 8.9ml of de-ionized water. Then, 46mg of $NaBH_4$ was added, the solution turned immediately from light yellow to yellow green. To that solution 10mg of catalyst was added. Concentration of 4-nitrophenol was recorded at 400nm in de-ionized water.

Figure 2.8. Aqueous solutions of 4-NP, MO and MB respectively.

Results and Discussion

3.1. Characterization of nanocatalysts

In the present work, the as-prepared CuO NPs were successfully synthesized *via* simple reduction method whereas γ-alumina supported copper and cobalt nanocomposites were fabricated *via* homogenous precipitation deposition (HDP) method. The as-fabricated nanocatalyst were then characterized through different analytical techniques like X-ray Diffraction (XRD), Scanning Electron Microscopy (SEM) and Thermogravimetric Analysis (TGA).

3.1.1. X-ray Diffraction (XRD) of nanocatalyst

The crystal type of all the as-obtained nanocatalysts were first characterized by XRD technique to determine their purity, phase formation and crystallinity. All the diffraction patterns obtained were compared with the reference JCPDS diffraction files.

3.1.1.1. XRD analysis of copper oxide NPs (Microwave Assisted method)

The typical XRD spectra for the as-synthesized mixed copper oxide NPs *via* Microwave Assisted method is shown in figure 3.1. The characteristic diffraction peaks located at 2θ values of 36.2°, 42.3° and 73.5° correspond to the miller indices (111), (200) and (311) respectively. These Bragg's reflections matched well with the Cu_2O planes with standard (JCPDS card # 01-080-3714). In addition, two diffraction peaks at 48.7° and 61.4° were due to (202) and (-113) reflection of CuO atomic planes respectively (JCPDS card # 10-0319).

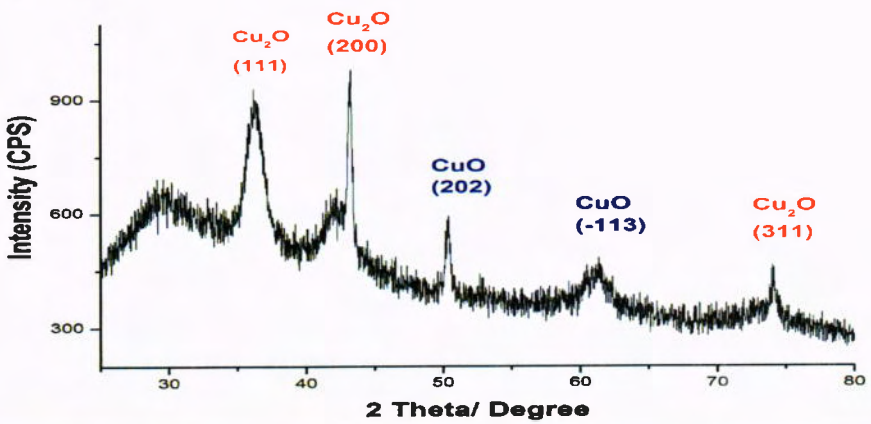

Figure. 3.1. XRD spectra of mixed copper oxide (CuO and Cu_2O) NPs

3.1.1.2. XRD analysis of CuO NPs (Simple Reduction method)

Figure 3.2 shows the XRD spectra of pure CuO nanoparticles which is in good agreement with the standard (JCPDS card No 10-0319). The characteristic peaks located at 2θ values of 32.45, 35.3, 38.6, 48.7, 53.6, 58.1, 61.4, 66.0, and 67.8 in the XRD spectra of CuO NPs can be indexed to the Bragg reflections of (110), (111), (-111), (-202), (020), (202), (-113), (-311), and (220) planes, respectively. Results revealed that copper is present in monoclinic CuO form whereas sharpness and broadening of XRD peaks demonstrated good crystallinity of the product. However, no peak corresponding to Cu_2O was observed which indicate the selective formation of CuO. The average crystalline size calculated by Debye Scherrer formula from the most intense diffraction index (111) was found to be ~ 29.00nm.

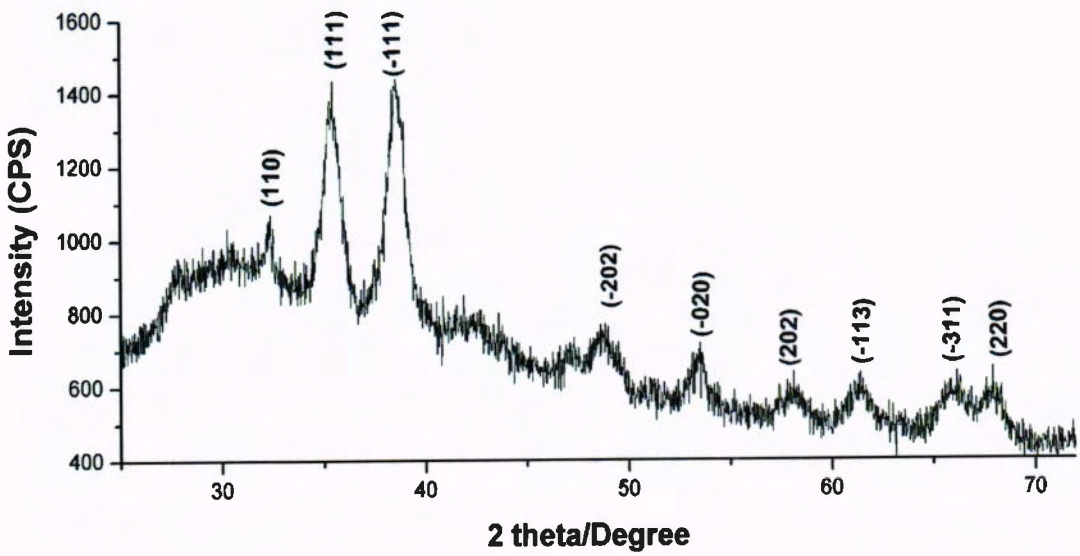

Figure 3.2. XRD spectra of pure CuO NPs

3.1.1.3. XRD analysis of γ –Alumina

Commercially available γ-alumina was used as catalytic support for transition metal nanocatalyst (CuO and Co_3O_2 NPs). The purity of the γ-alumina was confirmed by analyzing it by XRD. It is shown that three characteristic peaks at 37.2°, 45.9° and 67.2° are the Bragg's reflection of (311), (400) and (440) respectively, representing the crystallographic planes of γ-alumina (JCPDS card No 10-0425).

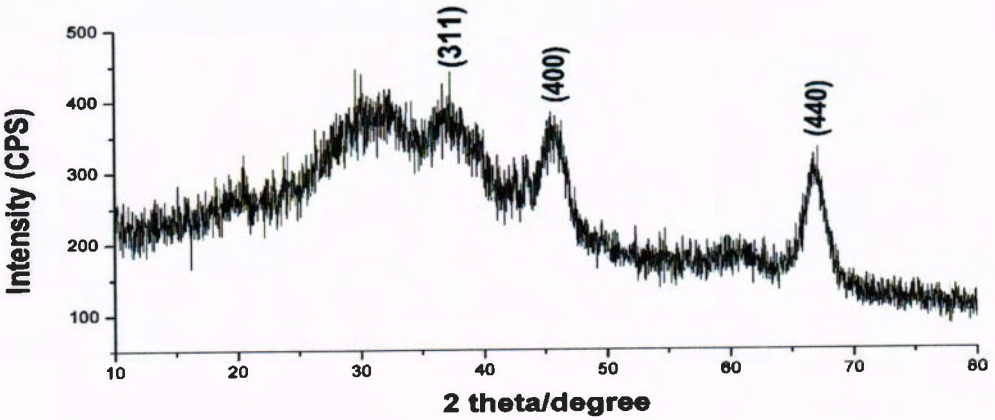

Figure. 3.3. XRD spectra of γ-alumina

3.1.1.4. XRD analysis of Cu/Al_2O_4 nanocatalyst

XRD pattern of Cu/Al_2O_4 calcined at 650 °C is shown in figure 3.4. Four characteristic peaks located at 2θ value of 31.4°, 36.9°, 59.6° and 65.3° correspond to (220), (311), (511) and (440) planes of Cu/Al_2O_4 respectively. (PDF file ICDD-78-1605). Broadening of the peak shows good crystallanity of the nanocatalyst. This indicates that Cu is present in CuO form, interacting strongly with the γ-Al_2O_3 support and converted into Cu/Al_2O_4 spinel phase by the solid phase reaction at 650 °C.

$$CuO + Al_2O_3 \longrightarrow Cu/Al_2O_4$$

It is clear from the literature that γ-Al_2O_3 has a spinal type structure in which oxygen atoms have a cubic close-packed arrangement creating defect sites in the alumina, thus copper ions are able to interact strongly and fill these defect sites at higher calcination temperature. In addition, calcination at higher temperature helps to increase atomic mobility and grain growth ensuring better crystallinity of the sample (delgado et al., 2012). The average crystalline size calculated by Debye Scherrer formula from the most intense diffraction index (311) was found to be ~ 29.1nm.

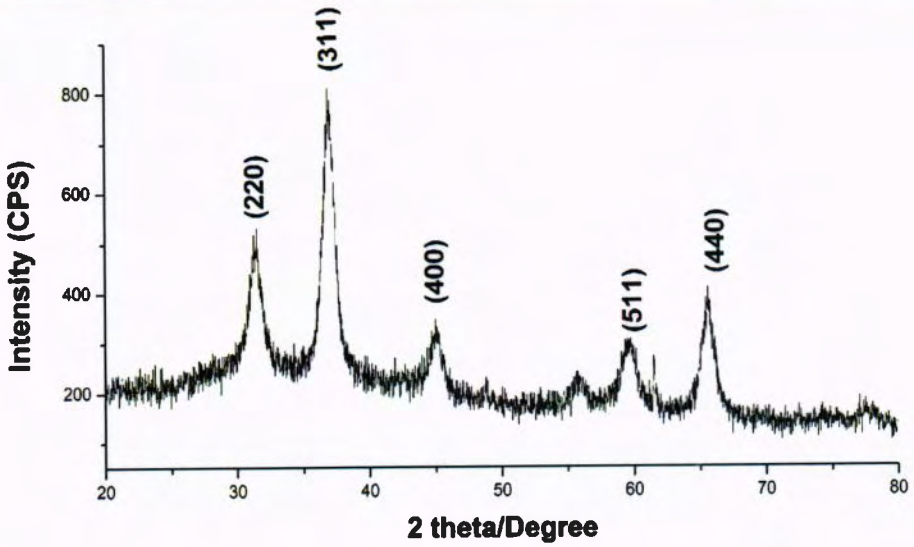

Figure 3.4. XRD spectra of Cu/Al_2O_4 nanocatalyst

3.1.2. Scanning Electron Microscopic (SEM) analysis of catalysts

The morphological studies of the as-prepared nanocatalysts were investigated by SEM at different resolutions.

3.1.2.1. SEM of CuO NPs

The surface topography and morphorology of CuO NPs are identified by SEM micrographs at different resolutions. (Figure 3.5)

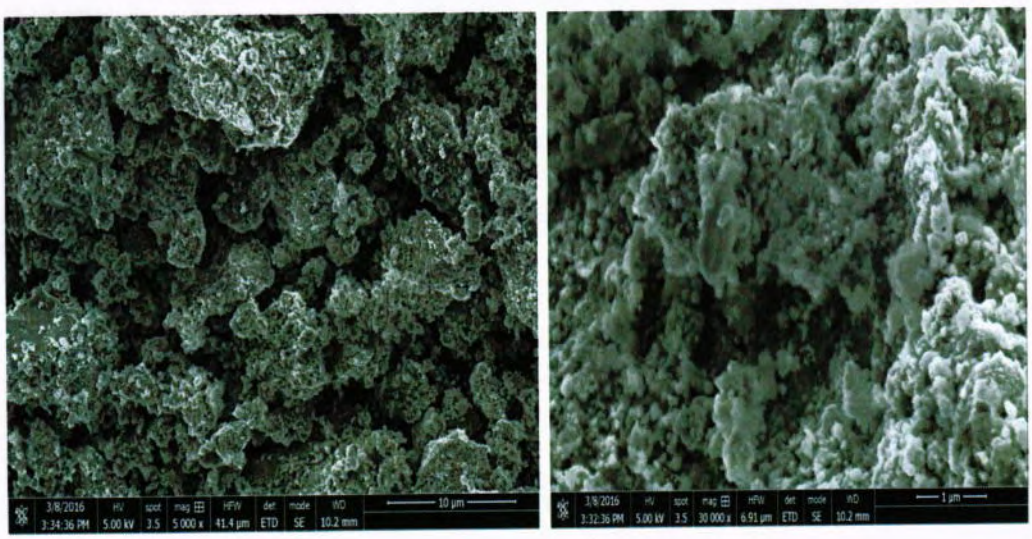

Figure 3.5. SEM micrographs of CuO NPS

The SEM images of CuO clearly show open porous structure of CuO nanoparticles in which material is composed of various tiny particles which are aggregated to form irregular shape/s (Deka, 2015).

3.1.2.2. SEM of Cu/Al_2O_4 nanocatalyst

Figure 3.6. shows the SEM micrograph of as-prepared nanocatalyst with Cu/Al_2O_4 spinel phase content at different resolutions. It is depicted from the SEM image that nanostructure of our catalyst is more porous due to the presence of CuO with the high spinel phase content of alumina. Because of the relatively low calcination temperature (650 °C), CuO remains porous and copper particles are present as discrete and agglomerated on the alumina support. However, it is reported by the Zhou et al., (2006) that catalytic activity can be enhanced by the pororus structure of the sample. Our results are consistent with the work of (Alipour et al., 2013) and (Torr et al., 2013).

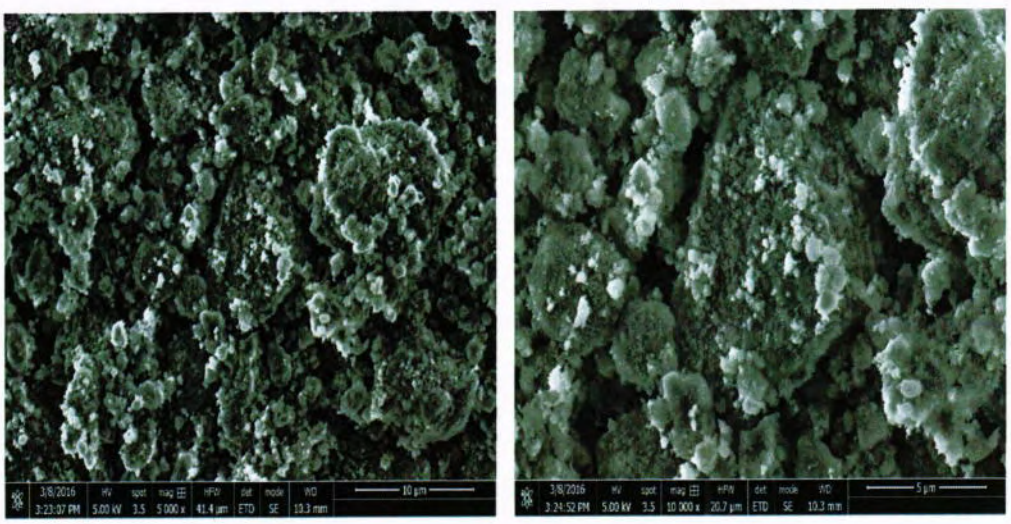

Figure 3.6. SEM micrographs of Cu/Al_2O_4

3.1.3. Thermogravimetric Analysis (TGA) of nanocatalyst

Thermal stability and mass changes study (weight loss/weight gain) of as obtained nanocatalysts were investigated through thermogravimetric analysis (TGA).

3.1.3.1. TGA of CuO NP

TGA curve for CuO NPs is shown in figure 3.7, where a total weight loss of only 0.15% is observed due to the loss of water which revealed the formation of pure metal oxide from its unreacted precursors. Minor weight loss indicates the thermal stability of the sample (CuO NPs) up to 500 °C (Park et al., 2015).

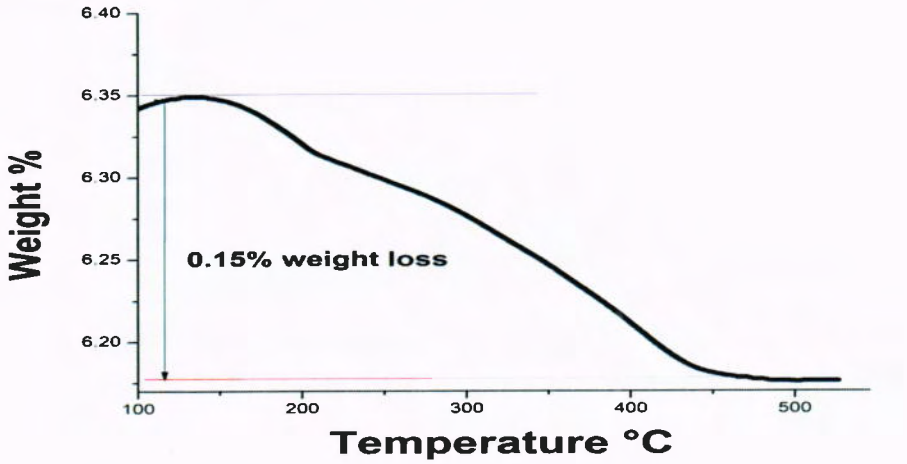

Figure 3.7. TGA curve of CuO NPs

3.1.3.2. TGA of Cu/Al_2O_4 nanocatalyst

The TGA curve of as-formed Cu/Al_2O_4 nanocomposite revealed the gradual weight loss steps from 90 to 750 °C with total weight loss of 6.5%. The decomposition follows the loss of physiosorbed and interlayer water molecules in the catalyst at 100 – 200 °C. The removal of hydroxyl layer and decomposition of reducing agent results in the destruction of layered structure between 200-750°C. However, no substantial weight loss revealed good thermal stability of our as synthesized Cu/Al_2O_4 nanocomposite at temperature upto 800°C. Our result matches well with the work of Lv et al., (2009) and Song et al., (2013).

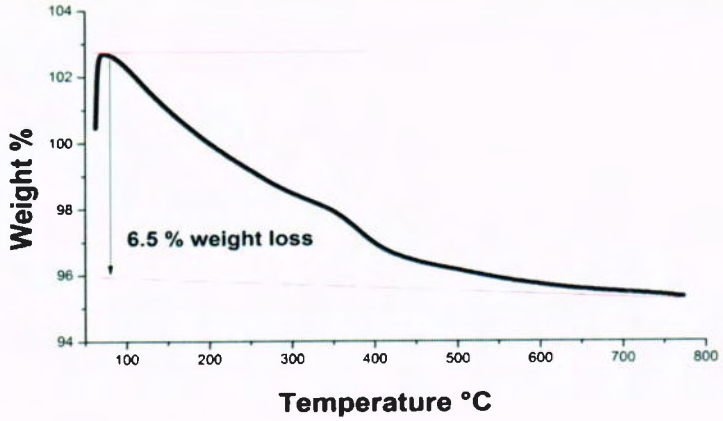

Figure 3.8. TGA curve of Cu/Al_2O_4 nanocomposite

3.2. Catalytic experiment

Recently, wastewater treatment using catalytic methods has been receiving significant attention worldwide. However, fewer studies have been reported in the literature on alumina based metal oxide nanoparticles as nanocatalyst for wastewater treatment especially, aromatic dyes and pollutants. In this study, series of experiments were performed to monitor the catalytic activity of as-synthesized CuO NPs and alumina based nanocatalysts ($Cu/Al_2O_4$and Co/Al_2O_4) separately, for the degradation of Methylene Blue (MB), Methyl Orange (MO) and 4-Nitrophenol (4-NP) as a model pollutant. In each catalytic experiment, a reaction mixture was prepared by adding 10 mg of catalyst in 10 ml of the respective dye solutions in the presence of oxidizing and reducing agents (H_2O_2 or $NaBH_4$) according to the respective reaction system.

The extent of dye degradation was confirmed by monitoring UV/vis absorption spectra by taking small aliquots from the reaction mixture after short time intervals (0, 8, 15, 30, and 45min) for each experimental set up to evaluate the time required for degradation. "0" minute spectrum was recorded just after the preparation of reaction solution. Reaction mixture was kept on continuous stirring during experiment and catalytic activity of different nanocatalyst was confirmed by the decrease in contaminant concentration as reaction time goes on. As a result, the combined absorbance spectra were plotted against wavelength (nm) for each experiment for the respective target dye pollutant. The activity of the nanocatalyst is expressed as the percent decrease in contaminant concentration

measured by absorption intensity. In general, Percent of the dye degradation rate was calculated after each experiment with the help of following equation;

$$\textbf{Degradation rate (\%)} = A_o - A_t / A_o * 100$$

A_o = Peak absorbance at 0 min

A_t = peak absorbance at reaction time (45 min) at the same wavelength for the dye solution.

3.3. Catalytic testing of nanoparticles

A comparative study was conducted to investigate the ability of various nanocatalysts (CuO NPS, $Cu/Al_2O_4$and Co/Al_2O_4) to decompose selected organic pollutants (MB, MO, and 4-NP) in the presence of oxidizing and reducing agents. First, a blank reaction (only dye solution and H_2O_2 or $NaBH_4$) was carried out to evaluate the role of catalysts in oxidative and reductive degradation.

3.4. Catalytic degradation of Methylene Blue

Methylene blue (MB) $C_{16}H_{18}N_3SCl$ is a polyaromatic synthetic dye with the molecular weight of 319.85g/mol. It is used as basic cationic dying materials in textile industry and also as staining agent to make certain body fluids and tissues make easier to view during various diagnostic exam such as on x-rays. It is water-soluble and non-biodegradeble whereas, acute exposure to MB can cause increased sweating, nausea, chest pain, stomach cramps and confusion. Among various experimental procedures, catalytic oxidation degradation is a highly preferable option to treat MB from the industrial waste streams.

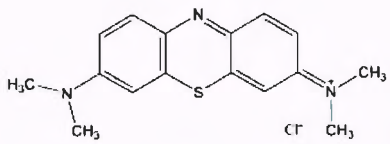

Methylene Blue

λ_{max} = 665nm

Herein, the oxidative degradation of MB was carried out in the presence of different nanocatalyst (CuONP's, Cu/Al_2O_4 and Co/Al_2O_4). A blank reaction (MB and H_2O_2) was

first set up to evaluate the role of catalyst in the oxidative degradation. A strong absorption peak at 665nm in Figure 3.9 indicates no degradation of MB even after 60 minutes of reaction time. Thus, verified the need of nanocatalyst in the reaction system to induce degradation because solitary hydroxyl radicals (OH°) generated in the presence of H_2O_2 are not enough to preceed degradation process of dyes.

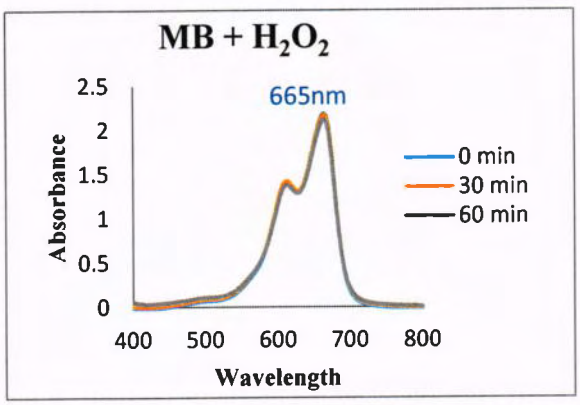

Figure 3.9. UV.vis spectra of blank reactions = MB solution (10ml) + H_2O_2 (2.5ml)

3.4.1. Oxidative degradation of MB with CuO NP's

To evaluate the catalytic effect of the support (γ-alumina), experiments based on copper oxide nanoparticles (CuO NPs) without support were carried out. For MB oxidative degradation, a reaction mixture was prepared by adding 2.5ml of H_2O_2 (30%) in 10ml of dye solution (0.06mM) along with the 10mg of CuO NP's at ambient conditions. However, reaction system was also setup in the absence of H_2O_2 to assess the role of oxidizing agent in degradation.

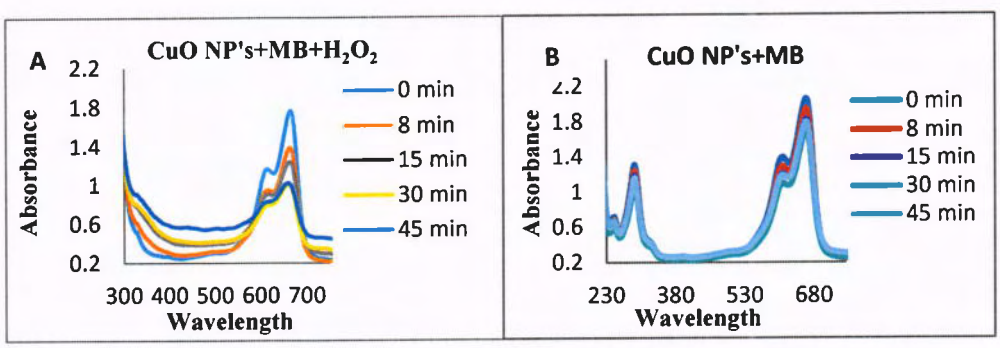

Figure 3.10. UV/vis spectra (A)= MB degradation by CuO NPs (10mg) with 10ml of MB solution in

the presence of 2.5ml H_2O_2. (B)= MB degradation by CuO NPs (10mg) with 10ml of MB solution in the absence of H_2O_2.

It is clear from figure 3.10 that recorded absorption spectra decreased gradually with the increase in reaction time which indicates the decomposition of MB molecules upto 40% with H_2O_2 and only 5% in the absence of H_2O_2 due to chemical stability of MB. Increased degradation in the presence of H_2O_2 along with the catalyst suggests that generated OH° radicals are required to react with the aromatic ring of the dye molecule to decolorize it partially or completely.

Moreover, original MB solution (without H_2O_2) shows four absorption peaks at 246, 292, 614 and 665nm as shown in fig 3.10 (B) due to strong absorption of dye molecules but after the addition of H_2O_2 in fig 3.10 (A), MB bands at 246 and 292nm were suppressed by the strong absorption of H_2O_2 (Deka et al., 2016).

3.4.2. Oxidative degradation of Methylene Blue with γ-alumina

Among the various catalytic supports, gamma alumina (γ-Al_2O_3) is cheap and most important active alumina studied widely as catalyst and catalyst support. Catalytic activity of the γ-alumina (without metal nanoparticles) was explained via probe reaction for oxidation of MB in the presence of H_2O_2. For this, a reaction mixture was prepared by adding 10mg of γ-alumina instead of CuO NP's while all the reaction conditions were same.

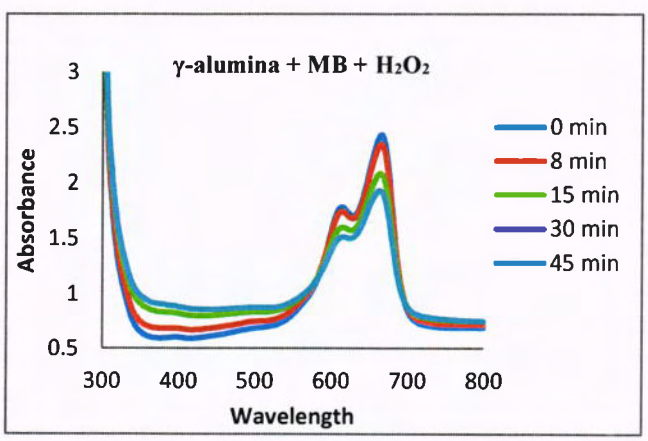

Figure 3.11. UV.vis spectra of γ-alumina (10mg) + 10ml of MB (0.06mM) + 2.5ml of H_2O_2

Fig. 3.11 displys the absorption spectra for the catalytic degradation of MB in the presence of γ-alumina (without nanoparticles). It represents only 15% MB removal in 45 minutes because of weak electrostatic interaction of dye molecule and γ-alumina. We assumed that, dyes usually physically adsorb onto the inert catalytic support such as γ-alumina, leading to the decolorization of wastewater. Adsorption does not help in breaking down the complex organic structures of the dye molecules into the nontoxic products such as CO_2 and H_2O.

After evaluating the role of bared nanoparticles (without support) and catalytic support (γ-alumina) in the oxidative degradation, the reaction rate was significantly enhanced by the slight modification of catalyst (deposition of transition metal oxide onto γ-alumina) *via* Homogenous Deposition Precipitation (HDP) method. This modification leads to the heterogenous catalyst system which is highly preferable due to its green credentials. It was very essential because metal oxide at nanoscale exhibit high catalytic activity due to their large surface to volume ratios but owing to high surface energy and narrow distribution, they get easily aggregated in aqueous media resulting in a remarkable decrease in their catalytic activity (Zhang et al., 2011). Thus, to efficiently use the metal nanoparticles as catalyst, they must be synthesized in specific morphologies or immobilized/stabilized onto certain inert/inorganic support to avoid agglomeration in the aqueous medium. In the current study, cupric oxide nanoparticles (CuO NPs) were deposited onto γ-alumina to further increase the degradation process of the organic aromatic pollutant. In addition, a heterogeneous nanocomposite based on cobalt oxide nanoparticles supported on γ-alumina was also synthesized. After that, catalytic activity of both nanocomposites (Cu/Al_2O_4 and Co/Al_2O_4) was compared against model pollutants (MB, MO and 4-NP) for their oxidative and reductive degradation.

3.4.3. Oxidative degradation of Methylene Blue with Cu/Al_2O_4

For the demonstration of oxidative degradation, the as prepared (Cu/Al_2O_4) nanocatalyst was added in the dye solution in the presence of 2.5ml of H_2O_2 (30%) At first, absorption spectrum was recorded at "0" minute just after the preparation of reaction solution and

then it was allowed to stir under ambient conditions till the next reading by drawing out 2ml of aliquots and analyzed through UV/vis spectroscopy.

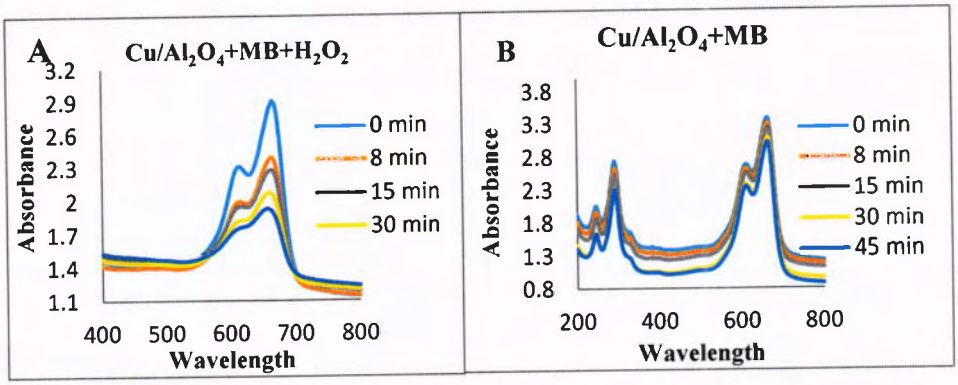

Figure 3.12. UV-vis spectra (A)= MB degradation by Cu/Al_2O_4 (10mg) with 0.06mM MB solution in the presence of 2.5ml H_2O_2. (B)= UV-vis spectra of similar reaction in the absence of H_2O_2.

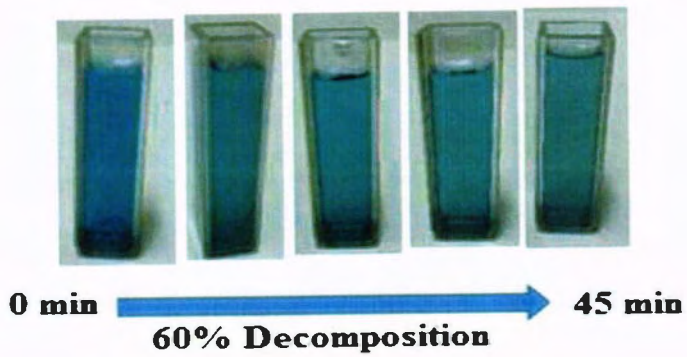

3.4.3.1. Kinetic study of MB decomposition

It is clear from the fig. 3.12 (A) that the absorbance peak for MB at 665nm decreased gradually with the increase in reaction time. It is also confirmed by observing the color of solution which starts fading and indicates gradual bleaching of the dye solution. 60% degradation was observed in 45 minutes in the presence of H_2O_2 on Cu/Al_2O_4. Superior catalytic degradation could be attributed to the positive synergistic effect of Cu/Al_2O_4 which demonstrates increased surface area to provide more active sites for oxidation reaction in the presence of H_2O_2 as compare to the unsupported CuO NPs. On the other hand; if reaction was set up in the absence of H_2O_2, results were quite dissimilar because of no degradation. Only 3% decolorization was recorded in the same reaction time. (Fig 3.12. B) The degraded quantity of the dye is proportional to the color loss of dye solution and reaction time. However, Decolorization/decomposition is accompanied with only

H_2O_2 as hydroxyl radical (OH°) are required for the oxidative degradation of the dye molecules

Compared with the results reported in literature, our catalyst system offers an efficient and active pathway for the oxidative degradation of MB. For example, Xia et al., 2014 conducted a research to evaluate the catalytic activity of Ti-based Layered Doubled Hydroxide against methylene blue. It was reported that degradation efficiency was 95% in 90 min under visible-light irradiation with initial dye concentration of 0.01mM. Similarly, Shimizu and co-workers in 2007 reported the 95% degradation efficiency after 60min reaction time in the presence of TiO_2 NPs together with ultrasound and H_2O_2. Thus, the most important aspect of our research is that no additional power input is required for oxidative degradation of MB in terms of sound, light or heat, other than simple stirring at room temperature

3.4.3.2. Possible mechanism for oxidative degradation of Methylene Blue

It has been stated that catalytic oxidation of MB in the presence of H_2O_2 and nanocatalyst conform the radical oxidative pathway. H_2O_2 is a powerful oxidizing agent to generate OH° and peroxide radicals when it decomposes in the presence of catalyst (Amini et al., 2015). Being heterogeneous, catalyst does not interact directly with the dye molecule in the reaction system. Production of hydroxyl radicals in the presence of H_2O_2 is the efficient and ultimate tool for the catalytic advance oxidation because it can break the chromophore/auxochrome which are responsible for the deep coloration of dyes, leading to their partial or complete degradation.

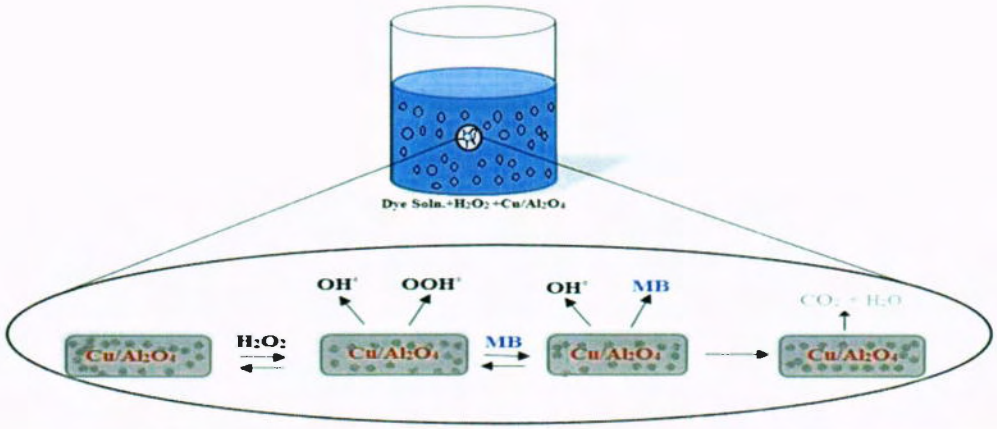

Figure 3.13. Adsorption-desorption mechanism of MB oxidation by H_2O_2 in the presence of Cu/Al_2O_4 nanocomposite.

The pathway behind the catalytic oxidation is that the dye molecule first adsorbs on the nanocatalyst surface where catalyst serves as an efficient electron transfer channel from oxidant to MB molecule to decompose aromatic ring/chromophores of the dye molecule. It is confirmed earlier from our results that Cu/Al_2O_4 nanohybrid with more surface area provide more active sites for adsorption of dye molecules as compared to the bare CuO NP's. And it is confirmed from the SEM results that CuO NPs are uniformly dispersed on the γ-alumina surface to catalyze H_2O_2 to generate free radicals such as OH°, OOH° and O_2^- which assist in oxidative degradation (Qu et al 2014). Peroxide first reacts on the active surface site of the catalyst leading to the adsorbed active specie and hydroxyl radicals at the same time interact with the MB molecules adsorbed on the catalyst surface, thus undergo oxidation reaction as shown in fig 3.13.

3.4.4. Degradation of Methylene Blue with Co/Al_2O_4 nanocatalyst

Cobalt based nanomaterials have shown more applications as compare to expensive metals in different sectors including degradation of organic water pollutants such as dyes and nitroaromatics using advance oxidation process.

To evaluate the catalytic activity of as-synthesized Co/Al_2O_4 catalyst for oxidative degradation of target pollutant (MB), a 10ml of MB solution (0.06mM) with 2.5ml of H_2O_2 was prepared. To which, 10mg of Co/Al_2O_4 nanocatalyst was added for each reaction system.

Oxidation degradation

For the oxidative degradation of MB, catalytic activity of Co/Al_2O_4 nanocomposite was investigated at both room temperature and slightly high temperature (50°C) at constant concentration of reactant (0.06mM) and nanocatalyst (10mg).

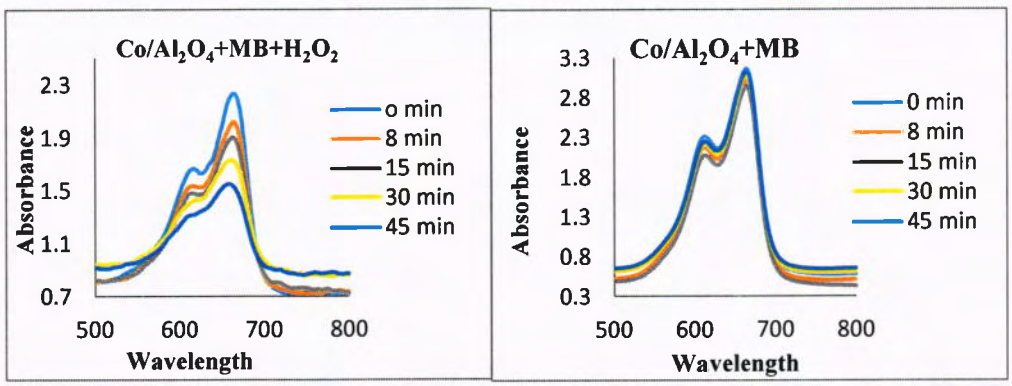

Figure 3.14. UV-vis spectra (A)= MB degradation by Co/Al_2O_4 (10mg) with 0.06mM dye solution in the presence of 2.5ml H_2O_2. (B)= UV-vis spectra of similar reaction in the absence of H_2O_2.

It is clear from the fig 3.14(A). that as the reaction time goes on at room temperature, the absorption peak of MB gradually decreased and it lead to 50% degradation in 45 min in the presence of H_2O_2. However, no degradation was obseverved when reaction was carried out in the absence of H_2O_2.

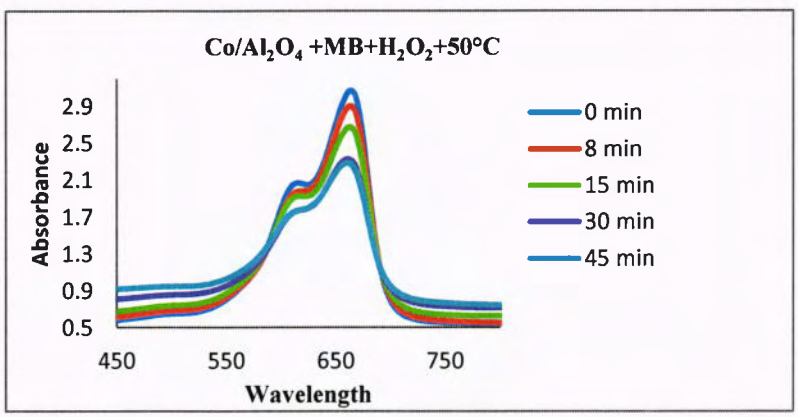

Figure 3.15. UV. vis spectra for MB+ Co/Al_2O_4 +H_2O_2+50 °C

On the other hand, when temperature of the experimnatal solution was increased upto almost 50 °C to check the effect of temperaure on oxidative degradation, a decrease in the removal efficiency was monitered as shown in figure 3.15. Only 20 % decolorization was recorded in 45 min. These results clearly negate the possibility of increased oxidative degradation at increased temperature.

3.5. Degrdation of Methyl Orange

Methyl orange (MO) $C_{14}H_{14}N_3NaO_3S$ is one of the anionic azo dyes with molecular weights of 327.33g/mol. It is commonly used in various chemical and textile industries and very toxic in nature. Its synthetic complex structure makes its degradation a difficult task (Jana et al., 2012 & Ai et al., 2011). Acute exposure to MO can cause increased heart rate, vomiting, shock, cyanosis, jaundice, gastrointestinal problems and tissue necrosis in humans (Yi et al., 2008).

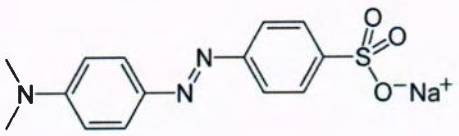

Methyl Orange

λ_{max} = 464nm

Effect of H_2O_2 on absorption spectra of Methyl Orange

Figure 3.16 displays the effect of H_2O_2 on absorption spectra of Methyl Orange. Original MO solution shows an absorption peak at 464nm, which is attributed to the conjugated structure linked by azo band. This azo band imparts very intense orange color to MO molecule.

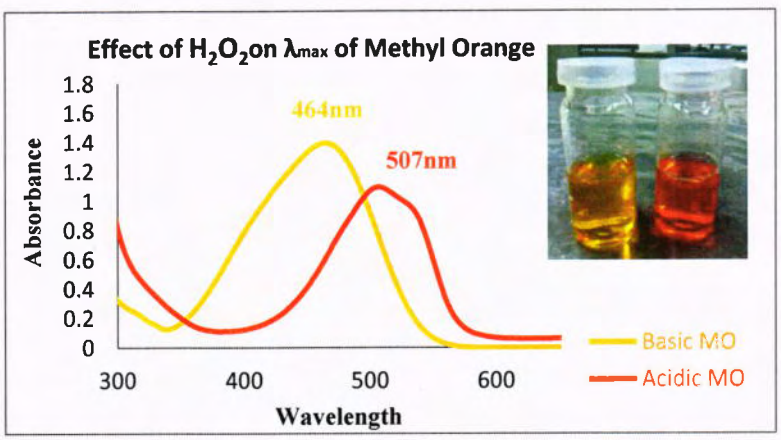

Figure 3.16. UV/vis spectra of MO under acidic and basic conditions. [inside showing the aqueous solutions of MO with H_2O_2 (red) and without H_2O_2 (orange)]

Original MO solution in water shows neutral pH (checked by pH paper) whereas on adding H_2O_2 its pH value is found to be <3, showing an acidic nature. Similarly, the color

of the MO solution oxidized by hydrogen peroxide also changes from orange to red and a bathochromic shift (wavelength increased 48 nm for MO) was observed from 464nm to 507nm attributed to the quinoide form of MO. It is obvious that shift in an absorption peak can be related to the change in the structure of MO molecule. This characteristic peak was chosen as a reference for monitoring the degradation of MO dye with H_2O_2 (Basahel et al., 2015).

pH>3.5

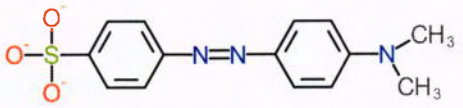

Azo structure

OH- ⇅ H

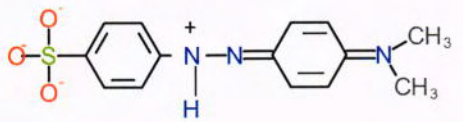

pH<3.5

Quinoide structure

Scheme 1. Structural changes of Methyl Orange under acidic and basic conditions.

Why we need catalyst for degradation??

A blank reaction (MO and H_2O_2) was first set up to evaluate the role of catalyst in the oxidative degradation. A strong absorption peak at 507nm in figure 3.17 indicates no degradation of MO even after 60 minutes of reaction time. Thus, verified the need of nanocatalyst in the reaction system to induce degradation because solitary hydroxyl radicals (OH°) generated in the presence of H_2O_2 are not enough to precede degradation process of dyes.

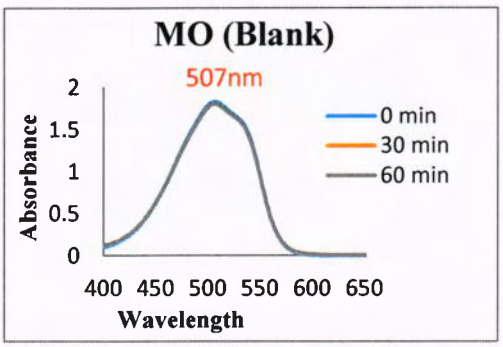

Fig 3.17. UV.vis spectra of blank reactions = MO dye solution (10ml) + H_2O_2 (2.5ml)

In the current study, degradation of MO was carried out in the presence of different nanocatalyst (CuONP's, Cu/Al_2O_4 and Co/Al_2O_4) separately.

3.5.1. Degradation of Methyl Orange with CuONP's

For oxidative degradation of MO, a reaction mixture was prepared based on MO solution in which 10mg catalyst (CuO NP's) and 2.5 ml of H_2O_2 was added.

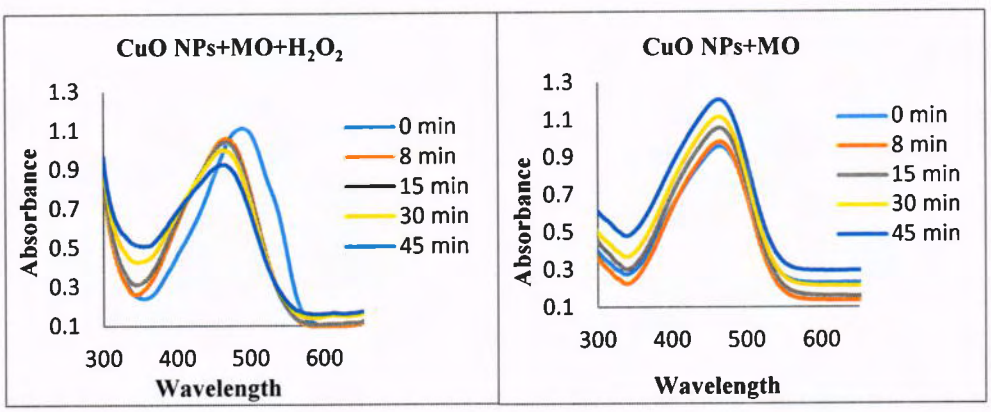

Fig. 3.18. UV/vis spectra (A)= MO degradation by CuO (10mg) with 0.06mM MO solution in the presence of 2.5ml H_2O_2. (B)= UV-vis spectra of similar reaction in the absence of H_2O_2.

It is mentioned earlier that a peak shift was observed for MO from 464nm to 507nm in the acidic medium by adding H_2O_2 due to protonation of dye molecule. Absorption spectra showed a slight decrease in the MO spectra in the presence of H_2O_2, reaction was completed in 45min with only 10% decomposition. On the other hand, a contrary behavior by MO was observed; the absorption spectra showed a gradual increase in absorbance as the reaction time proceed. This may be due to the decrease in catalytic activity associated with the aggregation of dye molecules in water which is explained in later section.

3.5.2. Degradation of MO with Cu/Al_2O_4

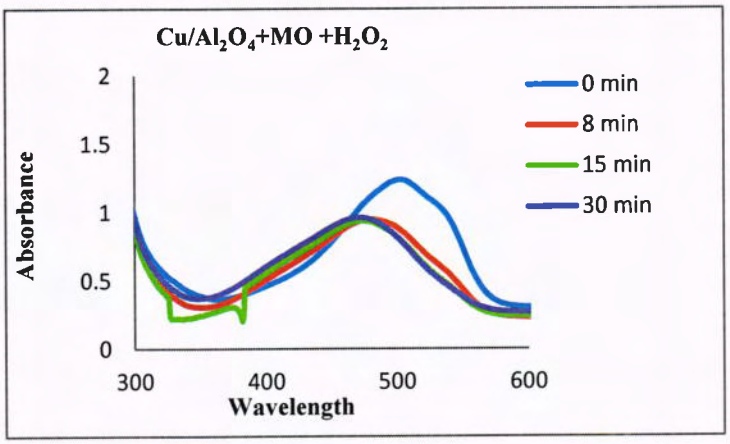

Figure. 3.19. UV-vis spectra for MO degradation by Cu/ Al_2O_4 (10mg) with 0.06mM dye solution in the presence of 2.5ml H_2O_2.

It is clear from the absorption spectra of MO oxidative degradation that only 20% degradation occurs in 30 minutes in the presence of H_2O_2. In addition, we are supposed to have a bathochromic shift (towards longer wavelength at 507 nm) for MO in the acidic medium by adding H_2O_2 which is apparent in the 0 min reading (just after preparing the experimental solution) nevertheless, this red shift showed a slight change in the spectral band position as it was at 489nm in the 45 min spectrum. However reaction was also set up in the absence of H_2O_2 but no decrease in MO concentration was observed.

3.5.2.1. Absorption spectral changes and Aggregation of MO dye molecules

Several possible explanations have been developed, but the most probable reason for the spectral changes (absorption/fluorescence) of MO oxidative degradation is the aggregation of dye molecule at the low concentration (10^{-5} – 10^{-4} M). (Buwalda et al 2001). Molecular interactions leading to the aggregation is one of the important features of organic dyes in aqueous media. It has been reported (Vylder & Keukeleire., 1978) that self-stacking of polar region of the individual monomers in dilute solutions of ionic dyes tend to form dimers or even many order aggregates and this process is affected by many factors such as complex structure, concentration of dye and the nature of solvent. Aggregation phenomena arises when molecular interaction between solute molecules become more favorable than the intermolecular interaction of solute and solvent. (Vara

and Ortis, 2016). Due to the self-aggregation, catalyst might be unable to break all the azo bond in MO molecules as these might not be accessible to the active surface sites of catalyst system. Thus as a result, dye failed to decompose even in the presence of nanocatalyst which lead to increased absorbance shown by the UV/vis spectra of MO degradation.

3.5.2.2. H-aggregates and J-aggregates

On the basis of molecular exciton theory of dipole dipole coupling, two types of the aggregation schemes have been summarized which may have different effects on the absorption spectra. H-aggregates are formed by the side by side stacking of the molecules or ions that create л-system in parallel fashion. As a result of H-aggregation, a blue shift is pronounced in which an absorption peak towards shorter wavelength (hypsochromic effect) is observed. On the other hand, head to tail aggregation is the characteristic signature of J-aggregates where red shift (bathochromic effect) is observed (Pastore and angelis, 2010)

Herein, we observed repeated contradictions in the absorption spectra of MO oxidation degradation with each catalyst system (CuONPs, Cu/ Al_2O_4, Co/ Al_2O_4). On the basis of aforementioned explanation, we concluded that aggregation of MO in aqueous medium results due to its complex structure and nature of solvent. In addition, spectral changes in figure 3.19 clearly showed H-aggregation of MO molecules due to slight hypsochromic effect. Absorption spectra of oxidized MO should be at 507nm which was obvious in 0 min spectra (just after the preparation of reaction mixture) but after 45 min contact time, λ_{max} was observed at 489nm However, organic solvent (ethanol) or addition of electrolyte (NaCl) can be used to overcome this problem but it is not a feasible alternativeto adopt with respect to the wastewater treatment.

So, we decided to investigate the catalytic activity of our as-prepared catalyst (Cu/Al_2O_4) under reductive environment by replacing H_2O_2 with $NaBH_4$, while all the other conditions were same. Moreover, Different experimental parameters were checked such as effect of temperature, dosage of reducing agent. Blank experiment (only $NaBH_4$ and

dye solution) was also conducted to better understand the co-relation of different parameters with catalyst activity.

3.5.2.3 Reductive degradation of Methyl Orange

As is well known, reduction of dye and organic contaminants occur only in the presence of metal nanoparticles and their color bleaching helps to determine the reduction kinetics based on the simple monitoring of spectroscopy measurements (Zhang et al., 2014). Dyes are ususally coloured because they absorb light in visible region (350-700nm). MO contains an azo bond with aromatic ring and sulphonic group that gives a sharp orange color to the dye molecule at 464nm. So, it is important to break the conjugate system of dye molecule to decolorize it by catalytic reduction reaction.

For the MO degradation, 1ml of $NaBH_4$ (0.1) was added in the reaction mixture (dye solution and catalyst). Reduction of MO was confirmed by the formation of new products, indicated by the strong absorption peak at 248nm.

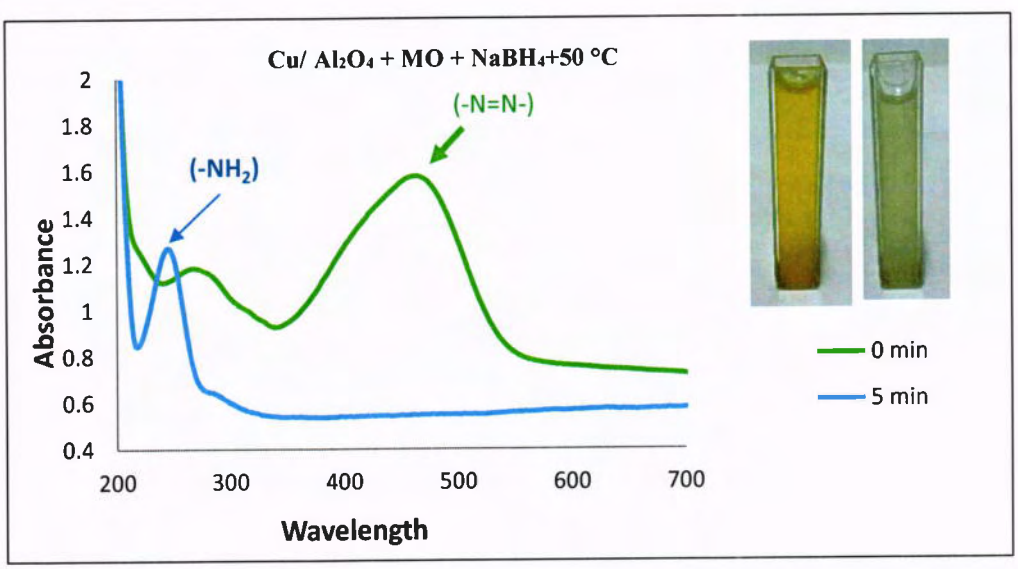

Figure 3.20. UV-vis spectra of MO degradation with 10 ml MO solution (0.06mM) in the presence of $NaBH_4$ at 50 °C. Inset showing the image of MO solution before (yellow) and after reduction (colorless)

At "0" min, no conversion was observed as indicated by strong absorption band of MO at 464nm, attributed to the λ_{max} of the azo bond (-N=N-) in the dye structure and responsible

for the intense orange color of the dye (Chakravarty et al 2015). After 5 min reaction time, experimental solution proceeded rapidly towards the complete decolorization indicating the breakdown of the (-N=N-) bond and it is confirmed by the straight line at 464nm as shown in figure 3.20. The formation of aromatic products was specified by the concomitant appearance of a new peak ~248 nm and the intensity of this absorption peak increased 5 min reaction time. This suggests successful decomposition of MO dye solution by the reduction of azo bond to two or more possible chemical structures with amine ($-NH_2$) functional group. The emergence of a new peak indicates that the decolorization of the dye was due to dye degradation from the solution in the presence of catalyst, instead of only physical adsorption (Sha et al, 2016)

Blank experiments (without catalyst) were performed at 50 °C and in the presence of excess $NaBH_4$ which ruled out the possibility of degradation without catalyst as no conversion occurred after 45min. Slight decrease in the UV-vis spectra may be due to the decolorization of the dye at temperature 50 °C as shown in Figure 3.21(A). On the other hand, no degradation was observed even in the presence of excess $NaBH_4$ (2.5ml), instead; aggregation of dye molecule was recorded in 45 min spectra. Figure 3.21(B)

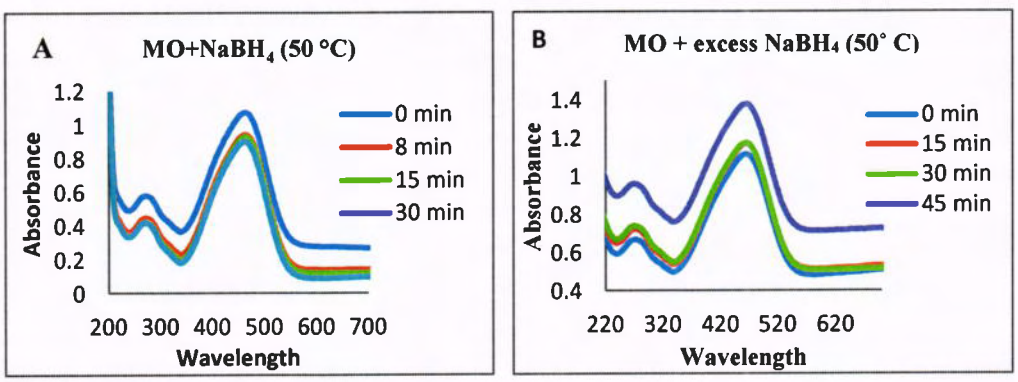

Figure 3.21.(A). UV-vis spectra of MO in the absence of Cu/Al_2O_4 catalyst at 50 °C. (B). UV.vis spectra of MO with excess $NaBH_4$

3.5.2.4. Possible mechanism for reductive degradation

During the reduction reactions, $NaBH_4$ in the presence of catalyst, decompose to generate microbubbles of H_2, which serve as the powerful reducing agent in the aqueous solution. (Wu et al., 2015). In addition to that, nanocatalyst (Cu/Al_2O_4) act as excellent facilitator in e- transfer to induce dye degradation

$$NaBH_4 \longrightarrow Na^+ + BH_4^-$$

$$BH_4^- \xrightarrow{2H_2O} 4H_2 + BO_2^-$$

It is clear from the Figure 3.21(A) that the MO degradation was negligible with only $NaBH_4$ added at 50 °C with no change in MO color after 30 mins because of no direct e-transfer between BH_4^- and dye molecule in the absence of catalyst. But when catalyst was added in the experiemntal solution, reaction was complet within only 5 minutes (Figure 3.20).

In the MO structure, two phenyl rings are bridged togather by an azo bond which are decompoed and reduced into single phenyl rings in the presence of catalyst (Hakamada et al., 2012). Catalytic reduction takes place on the Cu/Al_2O_4 surface which facilitate e-transfer (hydrogen atom) from the borohydride ions to the dye molecule subsquently leading to the cleaving of azo bond (-N=N-) which is responsible for toxicity and intense color of dye molecule. Fast catalytic activity of Cu/Al_2O_4 nanocatalyst lead to decolorization and reduction. Thus, it decomposes MO molecule into nontoxic amine products. The proposed two products are sulfanilic acid and N, N-dimethyl 1-4-phenylene diamine (Chakravarty et al., 2015).

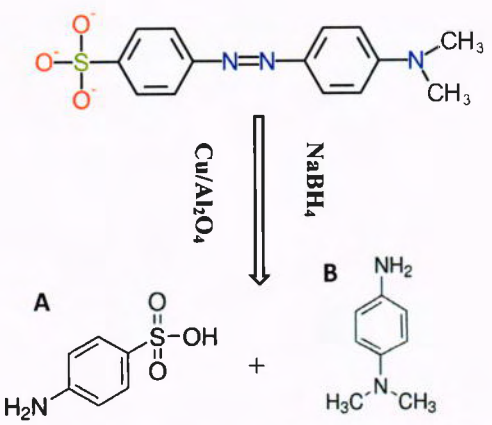

Scheme 2. Degraded products of MO (A). sulfanilic acid (B) N, N-dimethyl 1-4-phenylene diamine

Due to the complexity in oxidative degradation of MO, many studies have been reported on the reductive degradation of MO using relatively expensive metal nanocatalysts.

(Chong et al., 2016; Zhang et al., 2016 and Rajesh et al., 2014). Zheng et al, 2015 synthesized citrate capped silver nanoparticles *via* simple reduction method with silver nitrate and $NaBH_4$. The prepared nanoparticles were evaluated for the MO reduction degradation with $NaBH_4$ as reducing agent and concluded that orange color of MO gradually changed to colorless within 5 min. The concomitant increase in absorption peak at 250nm indicated the complete reduction of MO molecules. The degradation products were confirmed by Liquid chromatography-Mass spectrometric (LC-MS) analysis before and after degradation. MS spectra of their study clearly revealed that at 0 min reaction time, MS peak at m/z value of 306 represent original MO, after 5 min reaction time two peaks were recorded with m/z values of 195 and 136.1 which were consistent with the molecular weights of sodium sulafanilate and N, N-dimethyl 1-4-phenylene diamine, respectively. Thus, they concluded that Ag NPs are excellent nanocatalyst to effectively reduce MO into two non-toxic amine products (Zheng et al., 2015).

Recently, similar results have been reported by Charkravarty and coworkers in 2015. They testified Cu_2O nanoparticles decorated on the Amine factionalized graphite nanosheet for the reduction of MO in the presence of $NaBH_4$. Results showed that by adding the catalyst in the dye solution, reaction successfully proceeded towards complete reduction of MO in 17 min which is confirmed by formation of an absorbance peak at 250nm. On the basis of results, they proposed the mechanism for MO reduction which is explained by the electron transfer system of catalyst in the presence of $NaBH_4$ and thus, producing nontoxic products i.e., sulfanilic acid and N, N-dimethyl 1-4-phenylene diamine. Herein, we used cheap metal nanocatalyst (Cu/Al_2O_4 and Co/Al_2O_4) to reduce MO within 5 minutes.

3.5.3. Degradation of Methyl Orange with Co/Al_2O_4

The removal efficiency of as prepared Co/Al_2O_4 catalysts for MO was only 15% within 45 minutes. It showed very slow degradaton as we observe in case of Cu/Al_2O_4 nanocatalyst. So, due to the complex structure and decrease rate of degradation , we preferred to degrade MO in reducing medium in the presence of $NaBH_4$.

The catalytic activity of Co/Al_2O_4 catalyst for MO degradation in the presence of $NaBH_4$ was determined by spectroscopic measurements. Generally, chemical reactions are sensitive to a slight change in temperature and thus, it is an important factor to get an insight of the chemical reaction under investigation (Liou et al., 2005). In the present study, experiments for the MO reduction were carried out at 50 °C to check the effect of temperature on decolorization.

As shown in figure 24, no appreciable conversion of MO occur on Co/Al_2O_4 at room temperature in 45 min suggesting that reduction of MO is a thermodynamically controlled phenomena in which slightly higher temperature plays a significant role in preventing the dye aggregation as well as assisting in complete and rapid decolorization of MO.

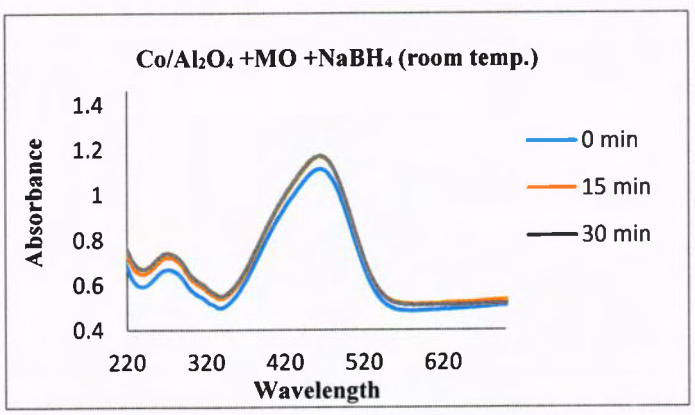

Figure 3.22. UV.vis spectra for MO reduction in the presence of $NaBH_4$ and Co/Al_2O_4 at room temperature. (25 °C).

Another reaction mixture for MO degradation was prepared with same reaction parameters but "0" min spectra was recorded after rising the temperature of the solution at 50 °C and keeping it constant throughout the experiment. It is clear from the figure 3.23 that with increasing temperature, conversion rate increased and reaction was completed in 5min where decline in the MO concentration was confirmed by the straight line at 464nm (λ_{max} for MO) and reduction products were represented by the strong absorption peak at 252nm and also the solution changed from bright yellow to colorless.

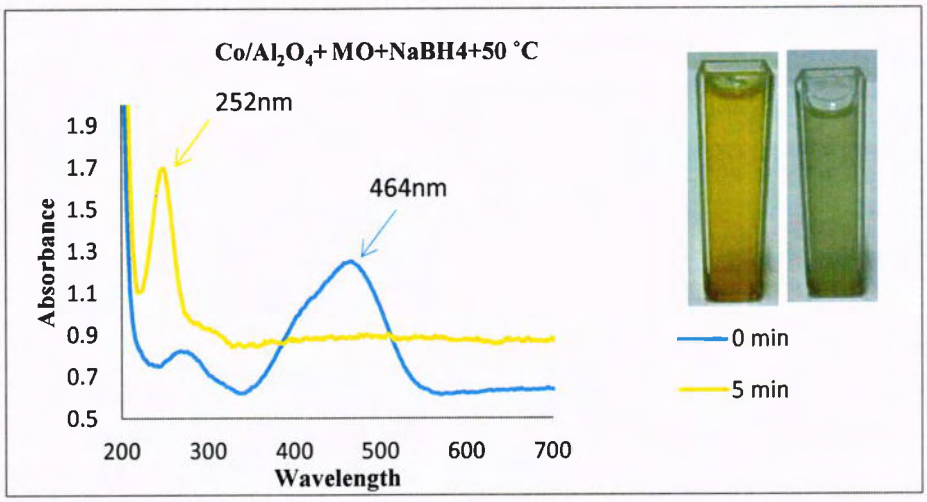

Figure 3.23. UV.vis spectra for MO reduction in the presence of $NaBH_4$ with Co/Al_2O_4 at 50 °C

Inset showing the image of MO solution at 0 min (yellow) and after 5 min (colorless).

Therefore, it can be concluded that high temperature leads to the rapid decolorization of MO by decreasing the reaction time and obviously increasing the degradation efficiency upto 100% within 5 min. Since, temperature of the industrial discharged effluent stream is consistently higher than room temperature; it is just feasible for the application of proposed route for the removal of MO.

Our reported results for MO reductive degradation are consistent with the work of Fan J and co-workers (2009) in which they successfully synthesized nanoscale zerovalent iron (NZVI) particles via liquid phase reduction method and their activity was focused on the reduction degradation of MO as a model pollutant. They evaluated the catalytic activity under different experimental parameters such as effect of temperature, pH, catalyst dosage and initial dye concentration. Results revealed that MO reduction rate increased significantly within 10 min from 72.2 to 93.8%, when the temperature of dye solution was raised from 20 °C to 40 °C at neutral pH and decreased with decreasing catalyst dosage and increasing dye concentration. In addition, degradation products were confirmed by Gas Chromatography-Mass spectrometric (GC-MS) analysis and they also proposed degradation mechanism; followed by the electron transfer process in the presence of $NaBH_4$.

Agglomeration is the key issue associated with the decreased catalytic activity of the pure metal oxide nanoparticles. In an experimental work by Mondal et al., 2015, cobalt nanoparticles were fabricated in the presence of surfactant such as Tertrabutyl Ammonium Bromide (TBAB) with a specific morphology named as spherical cobalt NPs to avoid aggregation. Their catalytic activity was investigated for the MO reduction with the initial dye concentration of 2×10^{-6} M in the presence of 1×10^{-4} M $NaBH_4$. It has been shown that absorption peak at 464nm decreased completely in 16 min. Moreover, they also concluded that the reduction rate was increased effectively at higher temperatures (50 °C) and pH < 8. Further, they highlighted the importance of transition metal oxide NPs such as cobalt NPs are superior to the catalytic activity of palladium NPs in reduction degradation of MO (Mondal, et al., 2015). It was studied that hollow cobalt nanoparticles offered a facile and efficient method to reduce MO into its respective amine products. Sha et al., prepared hollow cobalt nanoparticles using aluminum nanparticles as a template material by galvanic replacement reaction. The as-obtained nanocatalyst was used for the degradation of four azo dyes namely; amaranth, congo red, orange G and methyl orange. They found best results for reduction degradation, in which Co nanoparticles reacted with azo bond of MO and broke it into a single phenyl ring. (Sha et al., 2016).

3.6. 4-Nitrophenol

4-NP is one of the hazardous organic pollutants and has been widely used in manufacturing of insecticides, synthetic dyes, pharmaceuticals and to darken leather. Organic nitro compounds are usually converted into their respective amino products. Reduction product of 4-NP into 4-aminophenol (4-AP) is an important useful material in the synthesis of analgesics, antipyretic drugs, anticorrosion lubricants, and photographic developers (Pandey & Mishra., 2014). Reduction of 4-NP into 4-AP in the presence of nanocatalyst with excess of $NaBH_4$ is an active practice and feasible choice.

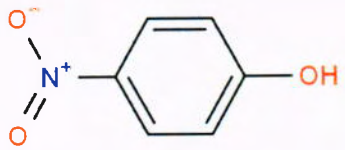

4-nitrophenol

λ_{max} = 317nm

The original aqeuous solution of 4-NP is light yellow in color with a characteristic UV/vis peak at 317nm. Reduction reaction started with the addition of $NaBH_4$ which changed the color of the solution from light to dark yellow indicating that 4-nitrophenol ions are dissociated into 4-nitrophenolate ions by the increasing the alkalinity of the solution (characteristic absorption peak at 400nm). Decline of this peak could suggest the conversion of 4-nitrophenol into 4-aminophenol with the absorption peak at 300nm. In this report, no change in the absorption spectra was observed when reaction was carried out in the absence of catalyst even after 60 min reaction time as shown in figure 3.24.This may be due to the high kinetic obstruction between the mutually repelling borohydride ions (BH_4^-) and 4-nitrophenolate ions ($C_6H_4NO_3^-$) in the absence of catlyst (Kumar and Deka, 2014). therefore we need a catalyst to start the reduction of 4-nitrophenol into 4-aminophenol.

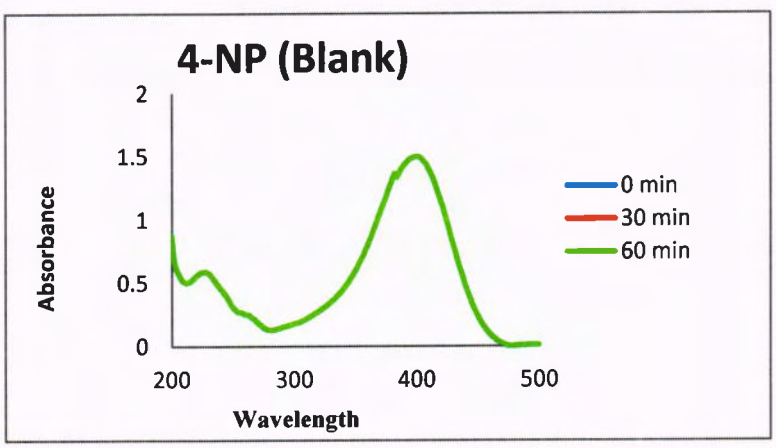

Figure 3.24 . UV.vis spectra of Blank 4-NP (without catalyst)

3.7.1. Reduction of 4-NP into 4-aminophenol with Cu/Al_2O_4

Herein, we reported the reduction of 4-NP into 4-aminophenol (4-AP) in the presence of $NaBH_4$ as a hydrogen source with Cu/Al_2O_4 as the nanocatalyst. For this, a reaction mixture was prepared by adding 10mg of Catalyst in 10ml of 4-NP solution (0.09mM) in the presence of 46mg $NaBH_4$. Figure 3.25 clearly indicates that as the reaction proceeded, the peak at λ_{max} = 400 nm corresponding to the p-nitrophenolate ion disappeared while concomitantly a new peak was observed at λ_{max} = 300nm within 60sec, a characteristic peak of 4-aminophenol, thus demonstrating the reduction of 4-nitrophenolate ion into 4-aminophenol and also the solution changed gradually from bright yellow to transparent.

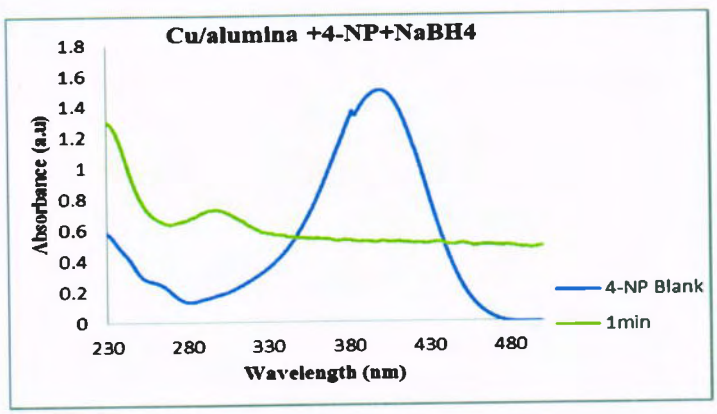

Figure 3.25. UV.vis spectra for 4-NP reduction in the presence $NaBH_4$ with Cu/Al_2O_4 nanocatalyst

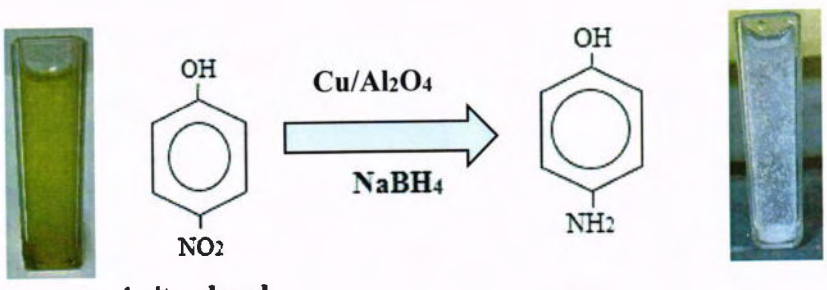

4-nitrophenol **4-aminophenol**

Scheme 3. Reduction of 4-NP into 4-AP

Proposed mechanism for 4-NP reduction

Figure 3.26. Schematic reduction of 4-NP into 4-AP by $NaBH_4$ in the presence of CuO NPs bound to Al_2O_3 support. The deocomposition of the sodium borohydride in the

presence of metal nanoparticles in aqueous media have been studied widely in the recent years. This is due to the ability of borohydride ions to generate hydrogen ions even at room temperature (Liu and Li, 2009). In addition, metal nanocatalyst act as elctron acceptor by gaining the charge from sodium borohydride.

In the present research, CuO NPs are dispersed onto the alumina surface and act as electron acceptor. Borohydride ions adsorb on the nanocatalyst surface rapidly and transfer active hydrogen species to the Cu/Al_2O_4 nanocomposite. 4-nitrophenolate ions

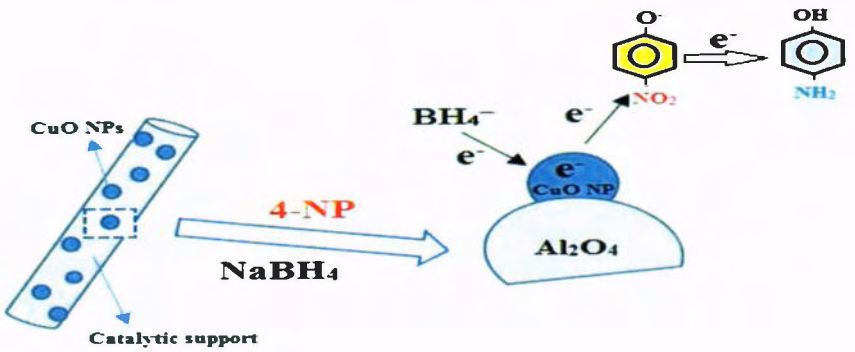

Figure 3.26. Schematic reduction of 4-NP into 4-AP by $NaBH_4$ in the presence of CuO NPs bound to Al_2O_3 support

are also adsorbed on the catalyst surface and this process is reversible i.e, it desorbs afterwards, when reduced into resultant product (4-AP). The reduction reaction proceeds by active hydrogen species from borohydrite and converting 4-NP into 4-AP by adding proton while removing oxygen. However, this adsorption/desorption process is assumed to take place rapidly at room temperature and controlled by Langmuir-Hinshelwood mechanism. Desorption of 4-AP creats free active site and the catalytic cycle can start again. (Wunder et al, 2010).

Moreover, excess of $NaBH_4$ was used to generate more BH_4^- ions that prevent the aerial oxidation of 4-NP and evolution of small hydrogen bubbles upon addition of $NaBH_4$ ensure the homogenous distribution of catalyst in the solution which is required for smooth reduction reaction (Noh et al., 2014)

3.7.3. Reduction of 4-NP with Co/Al_2O_4

Activity of as-prepared Co/Alumina catalyst was evaluated for the reduction of 4-nitrophenol into 4 –aminophenol in the presence of $NaBH_4$ as a reducing agent. In order to investigate the catalytic activity of Co/Alumina, a reaction mixture was prepared by adding 10mg of catalyst into 10ml (0.09mM) of 4-NP solution. Then, 46mg of $NaBH_4$ was added resulting in immediate color change from light to bright yellow corresponding to the formation of 4-nitrophenolate ions. Maximum absorption of 4-NP was recorded at 400nm. Later on, after adding Co/alumina catalyst, The bright yellow color of the solution gradually vanished just after the 60 sec reaction time, indicating the complete reduction of 4-NP into 4-aminophenol. Spectrum recorded just after the preparation of reaction mixture, was considered as "0" min spectrum. (Fig 3.27)

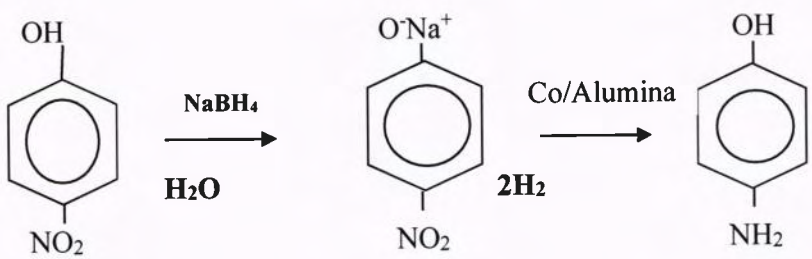

Scheme 3: Reduction scheme of 4-nitrophenol to 4-aminophenol

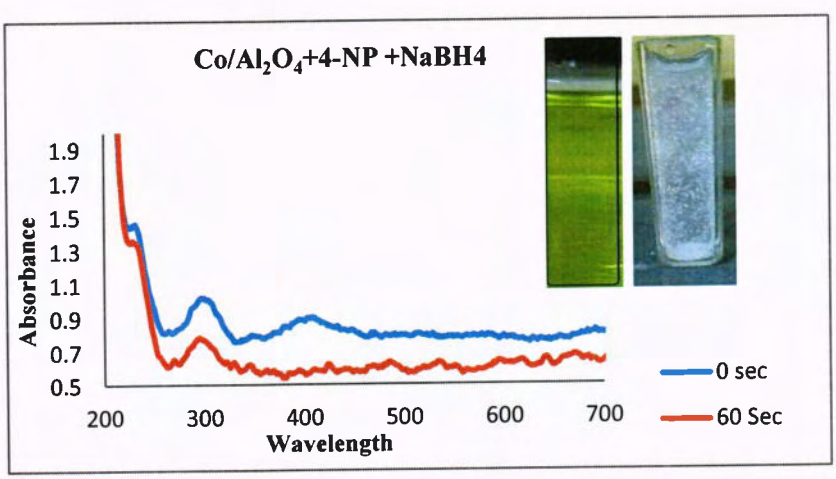

Figure 3.27. UV-vis spectra of 4-NP reduction by Co/Al_2O_4 in the presence of $NaBH_4$

3.8. Conclusion

In summary, we have successfully synthesized unsupported CuO NPs using an easy and environmentally benign chemical reduction method in the presence of sodium borohydride ($NaBH_4$) as reducing agent and γ-alumina based copper and cobalt nanocomposites were fabricated *via* Homogenous Deposition Precipitation (HDP) method in aqueous media. The as obtained nanoparticles were characterized through different analytical techniques such as X-ray Diffraction (XRD), Scanning Electron Microscopy (SEM) and Thermogravimetric Analysis (TGA) and evaluated as active nanocatalysts for wastewater treatment. In this report, we have selected aromatic dyes such as Methylene Blue (MB), Methyl Orange (MO) and 4-Nitrophenol (4-NP) as model pollutants for their oxidative and reductive degradation.

As a result of the porous structure of pure CuO NPs and high degree of dispersion of metal oxide (CuO, Co_2O_3) onto γ-alumina support, each catalytic system (CuO NPs, Cu/Al_2O_4 and Co/Al_2O_4) showed high rate of degradation reaction for selected pollutants. The activity of the nanocatalyst is expressed as the percent decrease in contaminant concentration after short time intervals (0, 8, 15, 30, and 45min) and represented by the combined absorbance spectra plotted against wavelength (nm) for each experiment. For oxidative degradation, hydrogen peroxide (H_2O_2) was used as a green oxidant and $NaBH_4$ was added for reductive degradation in the reaction mixtures. Blank reactions (without catalyst) were also performed to negate the possibility of degradation in the absence of catalyst.

In case of catalytic oxidative degradation, better decomposition was observed for MB in the order of 60% > 50% = 40% with Cu/Al_2O_4, Co/Al_2O_4 and CuO NPs respectively in 45 minutes in the presence of H_2O_2 because the generated hydroxyl radicals are capable of reacting with variety of organic compound leading to either partial or complete degradation. On the other hand, very slow (5%) degradation was reported without H_2O_2 after 45 minutes. Furthermore, only 10% decomposition of MO was recorded under

oxidative conditions due to its complex structure so it was tested for catalytic reductive degradation with $NaBH_4$.

In the presence of $NaBH_4$ under reductive medium, nanocatalysts (Cu/Al_2O_4 and Co/Al_2O_4) demonstrated excellent catalytic activity for MO degradation. Complete and rapid conversion was exhibited within 5 minutes at 50 °C. However, no degradation was observed when different experimental procedures (effect of temperature and excess of $NaBH_4$) were investigated for MO reduction reaction.

In case of 4-NP, catalytic reduction rates were remarkably high as 100% conversions were recorded within 60 seconds with each catalytic system (CuO NPs, Cu/Al_2O_4 and Co/Al_2O_4). In addition, possible mechanisms were also proposed for catalytic oxidative and reductive degradation. Finally, it is concluded that supported metal nanocatalysts demonstrate superior catalytic efficiency in term of both oxidative and reductive degradation in comparison to the unsupported one. Considering the simple preparation route, high catalytic potential and most importantly sustainable use of natural raw material (γ-alumina) as a host for various metal oxide nanoparticles make the heterogeneous supported metal nanocomposite that lead to new possibility as promising nanocatalysts for the industrial scale removal of aromatic pollutants and wastewater treatment.

3.9. Future perspective

Wastewater treatment and reuse is not new, and research on this global issue has evolved and advanced throughout human history. In this study, we have successfully synthesized supported and unsupported metal nanocatalyst and evaluated for the catalytic degradation of organic pollutants. This research was based on cost – effective and energy efficient catalytic system, however still need to highlight some aspect, related to the wastewater treatment.

1. To evaluate the activity of as-prepared nanocatalysts for the removal of other organic pollutants and azo dyes.
2. To synthesize new nanocatalyst by depositing transition metal/metal oxides on some support other than alumina.
3. To study the catalytic activity of nanocatalysts for the removal of heavy metals from the wastewater streams.

CHAPTER # 4

REFERENCES

References

1. Alipour, M., Nychka, A. J and Gupta, R. (2013). Evaluation of copper aluminum oxide as sorbents for high temperature air separation. *Energy and Fuels.* 28(1), 319-328.
2. Amini. M., Ashrafi, M., Gautam, and Chae, H. K. (2015). Rapid oxidative degradation of methylene blue by various metal oxides doped with vanadium. *RSC Advance*. 5, 37469-37475.
3. Alini, S., Bottino, A., Capannelli, G., Comite, A and Paganelli, S. (2005). Preparation and characterization of Rn/Al2O3 and their application in the adiponitrile partial hydrogenation and styrene hydroformylation. *Applied Catalysis A: General.* 292, 105-112.
4. Ai, L., Zhang, C. and Meng, L. (2011) Adsorption of methyl orange from aqueous solution on hydrothermal synthesized Mg−Al layered double hydroxide. J*ournal of Chemical and Engineering Data.* 56, 4217−4225.
5. Bafana, A., Dev, S. S and Chakrabarti, T. (2011). Azo dyes: past, present and the future. *Environmental Reviews*. 19, 350–370.
6. Bhattacharjee, A and Ahmeruzzaman, M. (2016). CuO nanostructure: facile synthesis and application for enhanced photodegradation of organic compounds and reduction of 4-nitrophenol in aqueous phase. *RSC Advance*. 6, 41348-41363.
7. Bottero. Y, J., Rose, J and Wiesner. R, M. (2005). Nanotechnologies: Tools for sustainable in a new wave of water treatment processes. *Integrated Environmental Assessment and Management.* 2(4), 391-395.
8. Buwalda, T. R and Engberts, N. J. (2001). Aggregation of dicationic surfactants with methyl orange in aqueous solution. *Langmuir.* 17, 1054-1059.
9. Chong, S., Zhang, G., Tian, H and Zhao, H. (2016). Rapid degradation of dyes in water by magnetic Fe°/Fe2O3/graphene composite. *Journal of Environmental Sciences.* 44, 148-157.
10. Cao, S., Tao, F. F., Tang, Y., Li, Y and Yu, J. (2016). Size and shape dependence catalytic performance of oxidation and reduction reaction on nanocatalysts. *Chemical Society Review*. 45, 4747-4765.

11. Carliell, C.M., Barclay, S.J., Shaw, C., Wheatley, A.D., and Buckley, C.A. (1998). The effect of salts used in textile dyeing on microbial decolorization of a reactive azo aye. *Environmnetal Technology*. 19(11), 1133–1137.
12. Chong, S., Zhang, G., Tian, H and Zhao, H. (2016). Rapid degradation of dyes in water by magnetic Fe°/Fe2O3/graphene composite. Hournal of Environmental Sciences. 44, 148-157.
13. Chakravarty, A., Bhowmik, K., Mukherjee, A and De, G. (2015). Cu2O nanoparticles anchored on amine-functionalized graphite nanosheet: A potential reusable catalyst. *Langmuir*.
14. Chequer, D, M. F., Oliveira, R, A. G., Ferraz, A, R. E., Cardoso, C. J., Zanoni, B< V. M and Oliveira, P. D. (2013). Textile Dyes: Dyeing process and environmental impact. *INTECH*. http://dx.doi.org/10.5772/53659.
15. Chirag, N. P. (2015). Nanotechnology: Future of environmental pollution control. *Internal Journal on Recent and innovation Trends in Computing and Communication.* 3(2), 164-166.
16. Dar, A. M., Nam, H. S and Kim, s. Y. (2010). Synthesis, characterization, and electrochemical properties of self-assembled leaf-like CuO nanostructure. *Journal of Solid State Electrochemistry.* 14, 1719-1726.
17. Deka, P., Deka, C. R and Bharali, P. (2016). Porous CuO nanostructure as reusable catalyst for oxidative degradation of organic water pollutants. *New Journal of Chemistry*. 40, 348-357.
18. Deng, D., Jin, Y., Cheng, Y., Qi, T and Xiao. (2013). Copper nanoparticles: Aqueous phase synthesis and conductive films fabrication at low sintering temperature. *Applied Material and Interfaces*. 5, 3839-3846.
19. Din, U. I., Shaharun, S. M., Subbarao, D and Naeem, A. (2014). Homogenous deposition precipitation method for synthesis of carbon nanofiber based Cu-ZrO2 catalyst for hydrogenation of CO2 to methanol. *Applied Mechanics and Materials*. 447, 83-84.
20. Deka, P., Deka, C. R and Bharali, P. (2016). Porous CuO nanostructure as reusable catalyst for oxidative degradation of organic water pollutants. *New Journal of Chemistry*. 40, 348-357.

21. Delgado, L. A., Fillali, L., Jimenez, A. J and Andres, L. S. (2012). Synthesis of α-alumina from a less common raw material. *Journal of Sol-gel Science and technology*. 64, 162-169.

22. Fan, J., Guo, Y., Wang, J and Fan, M. (2009). Rapid decolorization of azo dye methyl orange in aqueous solution b nanoscale zero-valent iron nanoparticles. *Journal of Hazardous Material*. 166, 904-910.

23. Fang, H., Wen, M., Chen, H., Wu, Q and Li, W. (2015). Graphene stabilized ultra-small CuNi nanocomposite with high activity and recyclability towards catalyzing the reduction of aromatic nitro-compounds. *Nanoscale.* 8, 536-542.

24. Glaspell, G., Fuoco, L and Shall, E, S. M. (2005). Microwave synthesis of supported Au and Pd nanoparticles catalyst for CO oxidation. The *Journal of Physical Chemistry B.*109. 17350-17355.

25. Gosh, B. K., Hazra, S., Naik, B and Ghosh, N. N. (2015). Preparation of Cu nanoparticles loaded SBA-15 and their excellent catalytic activity in reduction of variety of dyes. *Powder Technology*. 269, 371-378.

26. Hakamada, M., Hirashima, F and Mabuchi, M. (2012). Catalytic decolorization of methyl orange solution by nanoparous metals. *Catalysis Science and Technology*. 2, 1814-1817.

27. http://www.hydrogenlink.com/hydroxylradicalsreactivity.

28. Hameed, B. H.; Din, A. T. M.; Ahmad, A. L. (2007). Adsorption of methylene blue onto bamboo-based activated carbon: Kinetics and equilibrium studies. *Journal of Hazardous Material.* 141, 819–825.

29. Hildebrand, H., Mackenzie, K and Kopinke, D. F. (2009). Pd/Fe3O4 nano-catalysts for selective dehalogenation in wastewater treatment processes-Influence of water constituents. *Applied Catalysis B: Environmental*. 91, 389-396.

30. Horden, K. B. (2004). Chemistry of alumina, reaction in aqueous solution and its application in water treatment. *Advances in colloid and interface Science*. 110, 19-48.

31. Hua, L., Ma, H and Zhang, L. (2013). Degradation process analysis of the azo dyes by catalytic wet air oxidation with catalyst CuO/γ-Al_2O_3. *Chemosphere*. 90, 143-14.
32. Hu, H., Xin, H. J., Hu, H., Wang, X., Miao, D and Liu, Y. (2015). Synthesis and stabilization of metal nanocatalysts for reduction reaction – a review. Journal of Material Chemistry. 3, 11157-11182.
33. Herrera, E. J and Sakulchaichareon, N. (2009). Microscopic and spectroscopic characterization of nanoparticles. *In Drug delivery nanoparticle formulation and characterization.* 239-251. Ontario. Canada
34. Heide, D. P. (2011). X-ray photoelectron spectroscopy: An introduction to principles and practices. John Wiley & Sons. New Jersey. USA. DOI: 10.1002/9781118162897.
35. Horden, K. B. (2004). Chemistry of alumina, reaction in aqueous solution and its application in water treatment. *Advances in colloid and interface Science*. 110, 19-48.
36. Jana, D.; De, G. (2012). Controlled and stepwise generation of Cu2O, Cu2O@Cu and Cu nanoparticles inside the transparent alumina films and their catalytic activity. *RSC Advance*. 2, 9606–9613.
37. John, W. F and John, W. (2005). An introduction to surface analysis by XPS and AES. John Wiley & Sons. USA.
38. Joshi, M., Bhattacharyya, A and Ali, W. (2008). Characterization techniques for nanotechnology applications in textile. *Indian Journal of Fiber and Textile Research*. 33, 304-317.
39. Ju, S. K and Parales, E. R. (2010). Nitro aromatic Compounds, from Synthesis to Biodegradation. *Microbiology and Molecular Biology Rewievs*. 74(2). 250-272.
40. Khin, M. M., Nair, S. A., Babu, J. V., Murugan, B and Ramakrihna, S. (2012). A review on nanomaterials for environmental remediation. *Energy and Environmental Sciences*. 5, 8075-8109.

41. Karim, R. M., Rahman, A. M., Miah, J. A. M., Ahmed, H., Yanagisawa, M and Ito, M. (2011). Synthesis of γ-alumina particles and surface characterization. *The Open Colloide Science Journal.* 4, 32-36.
42. Kendrick, L. K and Gilkerson, R. W. (1986). State of aggregation of methyl orange in water. *Journal of Solution Chemistry.* 16(4), 257-267.
43. Liou, H. Y., Lo, L. S., Lin, J. L., Kuan, H. W and Weng, C. S. (2005). Chemical reduction of an unbuffered and buffered nitrate solution using catalyzed nanoscale iron nanoparticles. *Journal of Hazardous Materials B.* 127, 102-110.
44. Liu, H. B and Li, P. Z. (2009). A review: Hydrogen generation from borohydride hydrolysis reaction. *Journal of Power Source.* 187, 527-534.
45. Lv, W., liu, B., Qiu, Q., Wang, F., Luo, Z., Zhang, P and Wei, S. (2009). Synthesis, characterization and photocatalytic properties of spinel CuAl2O4 nanoparticles by a sonochemical method. *Journal of Alloys and compounds.* 479, 480-483.
46. Leng, Y. (2008). Material characterization: Introduction to microscopic and spectroscopic methods. Clementy loop, Singapore. John Wiley & Sons.
47. Moreau, M. L., ha, H, D., Zhang, H., Hovden, R., Muller, A. D and Rpbinson, D. R. (2013). Defining crystalline/amorphous phases of nanoparticles through X-ray absorption spectroscopy and X-ray diffraction: The case of nickel phosphide. *Chemistry of Materials.* 25, 2394-2403.
48. Ma, H., wang, H and Na, C. (2015). Microwave-assisted optimization of platinum-nickel nanoalloys for catalytic water treatment. Applied Catalysis B: Environmental. 163, 198-204.
49. Millennium Ecosystem Assessment (MA). 2005a. Ecosystems and Human Well-being: Synthesis. Island Press, Washington, DC.
50. Miyazaki, M and Islam, N. (2007). Nanotechnology systems of innovation-An analysis of industry and academia research activities. *Tec novation.* 27, 661-675.
51. Mott, D., Galkowski, J., Wang, L., Luo, J and Zhong, J. C. (2007). Synthesis of size-controlled and shaped copper nanoparticles. *Langmuir.* 23, 5740-5745.
52. Mondal, A., Adhikary, B and Mukherjee, D. (2015). Room temperature synthesis of air-stable cobalt nanoparticles and their use as catalyst for methyl orange dye

degradation. Colloids and Surfaces A: Physicochemical and Engineering Aspects. 482(5), 248-257.

53. Noh, J. and Meijboom, R. (2014). Reduction of 4-Nitrophenol as a Model Reaction for Nanocatalysis, in Application of Nanotechnology in Water Research (ed A. K. Mishra), John Wiley & sons, USA. doi: 10.1002/9781118939314.ch13.
54. Ndolomingo. J, M and Meijboom, R. (2015). Kinetic analysis of catalytic oxidation of Methylene blue over γ-alumina supported copper nanoparticles. *Applies Catalysis A: General.* 506. 33-43.
55. Ogugbue, C. J and Sawidis, T. (2011). Bioremediation and Detoxification of Synthetic Wastewater Containing Triarylmethane Dyes by Aeromonads hydrophila Isolated from Industrial Effluent. *Biotechnology Research International.* DOI 10.4061/2011/967925. Parlett, C., Wilon, K and Lee, F. A. (2013). Hierarchical porous materials: Catalytic applications. *Chemical Society Reviews.* 49, 3876-3893.
56. Ong, R, H., Hegde, G., Chigrinov, G. V and Khan, R. M. (2016). Sulfuric diazo dye stabilized copper nanoparticles compoite mixture: synthesis and characterization. *RSC Advance.* 6, 15094-15100.
57. Parlett, C., Wilon, K and Lee, F. A. (2013). Hierarchical porous materilas: Catalytic applications. *Chemical Society Reviews.* 49, 3876-3893.
58. Prasad, A, S. A and Rao, B, V. K. (2010). Physico chemical characterization of textile effluent and screening for dye decolorizing bacteria. *Global Journal of Biotechnology and Biochemistry.* 5(2), 80-86.
59. Prime, R. B., Bair, H. E., Vyazovkin, S., Gallagher, P. K and Riga, A. (2009). Thermgravemetric Analysis. (TGA). In Thermal Ananlysis of Polymers: Fundamental and Applications (eds J. D. Menczel and R. B. Prime), John Wiley & Sons. USA. doi: 10.1002/9780470423837.ch3.
60. Pandey, S and Mishra, B. S. (2014). Catalytic reduction of P-nitrophenol by using platinum nanoparticles stabilized by guar gum. *Carbohydrate Polymers.* 113, 225-231.

61. Pastore, M and Angelis, D. F. (2010). Aggregation of organic dyes on TiO2 in dye-sensitized solar cells models: *An ab Initio* Investigation. *ACS Nano*. 4(1), 556-562.

62. Park, H. S and Lee, J. W. (2015). Hierarchically mesoporous CuO/ carbon nanofiber coaxial shell-core nanowires for lithium ion batteries. *Scientific Reports*. 5(09754), 1-13.

63. Pozun, D. Z., Rodenbusch, E. S., Keller, E., Tran, K., Tang, W., Stevenson, J. K and Henkelman, G. (2013)A schematic investigation of P-Nitrophenol reduction by bimetallic dendrimer encapsulated nanoparticles. *The Journal of Physical Chemistry*. 117, 7598-7604.

64. Qu, J., Shi, L., He, C., Gao, F., Li, B., Zhou, Q., Hu, H., Shao, G., Wang, X and Qiu, J. (2014). Highly efficient synthesis of graphene/MnO2 hybrid and their application for ultrafast oxidative decomposition of methylene blue. *Carbon*. 66, 485-492.

65. Rajesh, R., Kumar, S and Venkatesan, R. (2014). Efficient degradation of azo dyes using Ag and Au nanoparticles stabilized on graphene oxide functionalized with PAMAM dendrimers. *New Journal of Chemistry*. 38, 1551-1558.

66. Rafatullaha, M., Sulaiman, O., Hashim, R and Ahmad, A. (2010). Adsorption of methylene blue on low-cost adsorbents: A review, *Journal of Hazardous Materials*, 177, 70–80.

67. Rajesh, R., Kumar, S and Venkatesan, R. (2014). Efficient degradation of azo dyes using Ag and Au nanoparticles stabilized on graphene oxide functionalized with PAMAM dendrimers. *New Journal of Chemistry*. 38, 1551-1558.

68. Sarkar, C and Dolui, K. S. (2015). Synthesis of copper oxide/reduced graphene oxide nanocomposite and its enhanced catalytic activity towards reduction of 4-nitrophenol. *RSC Advances*. 5, 60763-60769.

69. Simsikova, M., Bartos, M., Cechal, J and Sikola, T. (2015). Decolorizarion of organic dyes by gold nanoflowers prepared on reduced graphene oxide by tea polyphenol. *Catalysis Science and Technology*. 6, 3008-3017.

70. Sha, Y., Mathew, I., Cui, Q., Clay, M., Gao, F., Zhang, J. X and Gu, Z. (2016). Rapid degradation of azo dye methyl orange using hollow cobalt nanoparticles. *Chemosphere*. 144, 1530-1535.

71. Sharma, Y. C., Sriastava, V., Upadhyay, N. S and Weng, C. H. (2008). Alumina nanoparticles for the removal of Ni (II) from aqueous solutions. *Industrial and Engineering Chemistry Research*. 47. 8095-8100.

72. Sogand, A., Mohammad H and Samira, K. (2013). A comparative synthesis and physiochemical characterization on Ni/Al_2O_3-MgO nanocatalyst via sequential impregnation and sol-gel method used for CO_2 reforming of methane. *Journal of Nanoscience and Nanotechnology*. 13(7), 4872-4882.

73. Sha, Y., Mathew, I., Cui, Q., Clay, M., Gao, F., Zhang, J. X and Gu, Z. (2016). Rapid degradation of azo dyes methyl orange using hollow cobalt nanoparticles. *Chemosphere*. 144. 1530-1535.

74. Shimizu, N., Ogino, C., Dadjour, M. F and Murata, T. (2007). Sonocatalytic degradation of methylene blue with TiO2 pellets in water. *Ultrasonic Sonochemistry*. 14(2), 184-190.

75. Song, Q., Liu, W., Bohn, D. C., Harper, N. R., Sivaniah, E., Scott, A. S and Dennis, S. J. (2013). A high performance oxygen storage material for chemical lopping processes with CO2 capture. *Energy and Environmental Sciences*. 6, 288-298.

76. Tahir, A. M., Rasheed, H and Imran, S. (2010). Water quality status in rural area of Pakistan. PCRWR. Retreived December 12, 2015 from http://www.pcrwr.gov.pk/Btl_wr_report/Rural%20Areas%20Report/WQSReport.pdf.

77. Theron, J., Walker, A. J and Cloete. (2008). Nanotechnology and water treatment: applications and emerging opportunities. *Critical Reviews in Microbiology*. 34, 43-69.

78. Trueba,M and Trasatti, P. S. (2005). γ-Alumina as a support for catalysts: A review of fundamental aspects. *European Journal of Inorganic Chemistry*. 3393-3403.

79. Torr, D. F., Rosa, R. J., Kharisov, I. B and Ortiz, J. C. (2013). Preparation and characterization of Cu and Ni on alumina support and their use in the synthesis of low temperature metal-phthalocyanine using a parallel-plate reactor. *Materials.* 6, 4324-4344.

80. United Nation Children's Fund and World Health Organizatio Joint Monitering Programme for water supply and Sanitation (UNICEF and WHO). 2008. Progress on drinking water and Sanitation: Special Focus on Sanitation. UNICEF, New York and WHO, Geneva. 2008.

81. United Nation Industrial Development and Organization. (UNIDO). 2003. Industrial development report. Retrieved June 11, 2016 from https://www.unido.org/fileadmin/user_media/Publications/Pub_free/Industrial_development_report_2002_2003.pdf.

82. United Nations World Water Assessment Programme (UNWWAP). (2009). United Nations World Water Assessment Programme. The World Water Development Report 3: Water in a Changing World. UNESCO: Paris, France. Retrieved December 17, 2009 from http://www.unesco.org/water/wwap/wwdr/wwdr3/.

83. United Nations World Water Assessment Programme (UN WWAP). Water and Industry. Retrieved December 16, 2015 from http://www.unesco.org/water/wwap/facts_figures/ water_industry.shtml.

84. Vartooni, R. A., AliZadeh, M and Bagherzadeh, M. (2015). Green synthesis, characterization and catalytic activity of natural bentonite-supported copper nanoparticles for the solvent-free synthesis of 1-substituted 1H-1,2,3,4-tetrazoles and reduction of 4-nitrophenol. Beilstein Joural of Nanotechnology. 3(6), 2300-2309.

85. Vyazovkin, S. (2012). Thermogravimetric Analysis. *Characterization of Material.* 1-12. John Wiley & Sons. USA.

86. Vara, J and Ortiz, S. C. (2016). Thiazine dyes: Evaluation of monomeric and aggregate forms. *Spectrochimica Acta Part A: Molecular and Biomolecular Spectrocopy.* 166, 112-120.

87. Wunder, S., Polzer, F., Lu, Y., Mei, Y and Ballauff, M. (2010). Kinetic analysis of catalytic reduction of 4-nitrophenol by metallic nanoparticles immobilized in spherical polyelectrolyte brushes. *Journal of Physical Chemistry C.* 114, 8814-8820.

88. World Health Organization (WHO). 2002. World Health Report: Reducing Risk, Promoting Healthy Life. France. Retrieved December 3, 2015 from http://www.who. Int/whr/2002/en/whr02_en.pdf.

89. Wu, H. and Chen, H. D. (2004). Synthesis of high- concentration Cu nanoparticles in aqueous CTAB solutions. *Journal of Colloid and interface Science*. 273, 165-196.

90. Wang, H., Xu, Z. J., Zhu, J. J and Chen, Y. H. (2002). Preparation of CuO nanoparticles by microwave irradiation. *Journal of Crystal Growth.* 244, 88-94.

91. Wu, C., An, X Gao, S and Su, L. (2015). Self-assembly of cuprous oxide nanoparticles supported on reduced graphene oxide and their enhanced performance for catalytic reduction of nitrophenol. *RSC Advance*. 5, 71259-71267.

92. Wang, S., Zhang, J., Yuan, P and Xu, Q. (2015). Au nanoparticles decorated N-containing polymer spheres: additive free synthesis and remarkable catalytic behavior for reduction of 4-nitropheonl. Journal of Material Science. 50(3), 1323-1332.

93. Wang, H., Xu, J., Zhu, j and Chen, H. (2002). Preparation of CuO nanoparticles by microwave irradiation. *Journal of Crystal Growth.* 244. 88-94.

94. Wu, H. S and Chen, H. D. (2004). Synthesis of high-concentration Cu nanoparticles in aqueous CTAB solutions. *Journal of Colloid and Interface Sciences*. 273, 165-169.

95. Xu, D., Cheng, F., Lu, Q and Dai, P. (2014). Microwave enhanced catalytic degradation of methyl orange in aqueous solution over CuO/CeO2 catalyst in the absence and presence of H2O2. *Industrial & Engineering Chemistry Research.* 53, 2625-2632.

96. Xia, S. J., Liu, F. X., Ni, Z. M., Shi, W., Xue, J. L and Qian, P. P. (2014). Ti-based layered doubled hydroxides: efficient photocatalysts for azo dyes degradation under visible light. *Applied Catalysis B: Environmental.* 144, 570-579.

97. Yand, M amd He, J. (2011). Fine tuning of the morphology of copper oxide nanostructure and their application in ambient degradation of methylene blue. *Journal of Colloid and interface Science.* 355, 15-22.

98. Yi, J and Zhang, L. (2008). Removal of methylene blue dye from aqueous solution by adsorption onto sodium humate/polyacrlamide/clay hybrid hydrogels. *Bioresource Technology.* 99, 2182–2186.

99. Yang, L., Luo, S., Li, Y., Xiao, Y., kang, Q and cai, Q. (2010). High efficient photocatalytic degradation of p-nitrophenol on a unique Cu2O/TiO2 p-n heterojunction network catalyst. *Environmental Science and Technology.* 44, 7641.

100. Zhang, G., Wang, S., Zhao, S., Fu, L., Chen, G and Yang, F. (2011). Oxidative degradation of azo dyes by hydrogen peroxide electro generation in situ on anthraquinonemonosulphonate/polypyrrole composite cathode with herterogeneous CuO/ γ-Al2O3 catalyst. *Applied Catalysis B: Environmental.* 106, 370-378.

101. Zhou, L., Gao, C and Xu, W. (2010). Magnetic dendritic materials for highly efficient adsorption of dyes and drugs. *Applied materials and interfaces.* 2(5), 1483-1491.

102. Zhou, Z., Lu, C., Wu, X and Zhang, X. (2013). Cellulose Nanocrystals as a novel support for CuO nanoparticles catalysts: facile synthesis and their application to 4-nitrophenol reduction. RSC Advance. 3, 26066-26073.

103. Zhu, M., M, D., W, C., Di, J and Diao, G. (2013). Degradation of methylene blue with H2O2 over a cupric oxide nanosheet catalyst. *Chinese Journal of Catalysis.* 34, 2125-2129.

104. Zheng, Q. L., yu, D. X., Xu, J. J and Chen, Y. H. (2015). Reversible catalysis for the reaction between methyl orange and NaBH4 by Ag nanoparticles. *Chemical Communications.* 51 (6), 1050-1053.

105. Zhou, K., Wang, R., Xu, B and Li, Y. Synthesis, characterization and catalytic properties of CuO nanocrystals with various shapes. *Nanotechnology* 2006, 17, 3939–3943.

106. Zhang, P., Changlu, S., Zhang, Z., Zhang, M., Mu, J., Guo, Z and Liu, Y. (2011). In situ assembly of well-dispersed Ag nanoparticles (AgNPs) on electrospun carbon nanofibers (CNFs) for catalytic reduction of 4-nitrophenol. *Nanoscale.* 3, 3357-3363.

107. Zhang, P., Sui, Y., Wang, C., Wang, Y., Cui, G., Wang, c., Liu, B and Zou, B. (2014). A one-step green route to synthesize copper nanocrystals and their application in catalysis and surface enhanced Raman scattering. *Nanoscale.* 6, 5343-5350.

108. Zhang, Y., Gao, F., Wanjala, B., Li, Z., Cernigliaro, G and Gu, Z. (2016). High efficiency reductive degradation of a wode range of azo dyes by SiO2-Co core-shell nanoparticles. *Applied Catalysis B: Environmental.* 199, 504-513.